

This article was downloaded by:

On: 23 January 2011

Access details: *Access Details: Free Access*

Publisher *Taylor & Francis*

Informa Ltd Registered in England and Wales Registered Number: 1072954 Registered office: Mortimer House, 37-41 Mortimer Street, London W1T 3JH, UK



## Journal of Coordination Chemistry

Publication details, including instructions for authors and subscription information:

<http://www.informaworld.com/smpp/title~content=t713455674>

### Electrons and Ions Moving Across Liquid Membranes

Giancarlo De Santis<sup>a</sup>; Michela Di Casa<sup>a</sup>; Luigi Fabbrizzi<sup>a</sup>; Alberto Forlini<sup>a</sup>; Maurizio Licchelli<sup>a</sup>; Carlo Mangano<sup>a</sup>; Ján Mocák<sup>a</sup>; Piersandro Pallavicini<sup>a</sup>; Antonio Poggi<sup>a</sup>; Barbara Seghi<sup>a</sup>

<sup>a</sup> Dipartimento di Chimica Generale, Università di Pavia, Pavia, Italy

**To cite this Article** De Santis, Giancarlo , Casa, Michela Di , Fabbrizzi, Luigi , Forlini, Alberto , Licchelli, Maurizio , Mangano, Carlo , Mocák, Ján , Pallavicini, Piersandro , Poggi, Antonio and Seghi, Barbara(1992) 'Electrons and Ions Moving Across Liquid Membranes', *Journal of Coordination Chemistry*, 27: 1, 39 – 73

**To link to this Article:** DOI: 10.1080/00958979209407943

**URL:** <http://dx.doi.org/10.1080/00958979209407943>

PLEASE SCROLL DOWN FOR ARTICLE

Full terms and conditions of use: <http://www.informaworld.com/terms-and-conditions-of-access.pdf>

This article may be used for research, teaching and private study purposes. Any substantial or systematic reproduction, re-distribution, re-selling, loan or sub-licensing, systematic supply or distribution in any form to anyone is expressly forbidden.

The publisher does not give any warranty express or implied or make any representation that the contents will be complete or accurate or up to date. The accuracy of any instructions, formulae and drug doses should be independently verified with primary sources. The publisher shall not be liable for any loss, actions, claims, proceedings, demand or costs or damages whatsoever or howsoever caused arising directly or indirectly in connection with or arising out of the use of this material.

# ELECTRONS AND IONS MOVING ACROSS LIQUID MEMBRANES

GIANCARLO DE SANTIS, MICHELA DI CASA, LUIGI FABBRIZZI,\*  
ALBERTO FORLINI, MAURIZIO LICCHELLI, CARLO MANGANO,  
JÁN MOCÁK,† PIERSANDRO PALLAVICINI, ANTONIO POGGI  
and BARBARA SEGHI

*Dipartimento di Chimica Generale, Università di Pavia, via Taramelli 12, 27100 Pavia, Italy*

*Dedicated to Professor Piero Paoletti, University of Florence, Italy, on the occasion of his 60th birthday*

Oxidation and reduction reactions can be carried out by interfacing the aqueous solution containing the reducing agent and the aqueous solution containing the oxidizing agent by a layer of a water immiscible solvent (e.g.  $\text{CH}_2\text{Cl}_2$ , the liquid membrane): in the membrane a lipophilic redox system C has to be present, which transports electrons from the aqueous reducing phase to the aqueous oxidizing phase and, in its oxidized form  $\text{C}^+$ ,  $\text{X}^-$  anions in the opposite direction. Metal complexes have been tested as carriers for the transport of electrons across liquid membranes. In particular, transition metal complexes of lipophilic versions of cyclam and 2,2'-bipyridine have been investigated. The three-phase redox processes can be controlled by varying the potential of the  $\text{C}/\text{C}^+$  couple in the  $\text{CH}_2\text{Cl}_2$  solution. Further selectivity effects derive from the kinetics of the electron transfer process at the membrane/aqueous phase interface. The possibility to perform light driven electron transport processes mediated by a metal centred carrier is discussed.

## 1. LIQUID MEMBRANES: A USEFUL TOOL IN SEPARATION SCIENCE AND TECHNOLOGY

A membrane is a permeable barrier which separates two phases. Permeability to different chemical entities may be selective, which makes membranes a useful tool to separate and purify substances.<sup>1</sup> A water immiscible liquid interfacing two aqueous layers may act as a liquid membrane. Figure 1 reports some simple glassware used to prepare liquid membrane devices: in the case described, the immiscible liquid is heavier than water (e.g.  $\text{CH}_2\text{Cl}_2$ ,  $\text{CHCl}_3$ ). One of the aqueous layers (the source phase) may contain some chemical objects we are interested to transport to the other aqueous layer (the receiving phase). To do that, we need the help of a chemical system, the carrier, dissolved in the liquid membrane, prone to interact with the chemical object of interest at the source phase/membrane interface and to extract it into the water immiscible layer. Thus, the "carrier-object" complex will diffuse to the other side of the membrane: here, the object may be released to the aqueous receiving phase, provided that the overall process involves an energy gain. In other words, the transport of a chemical object from the source phase to the receiving one goes on if an appropriate potential gradient exists between the two phases.

\* Author to whom correspondence should be addressed.

† On leave from the Department of Analytical Chemistry, Slovak Technical University, Bratislava, Czechoslovakia.

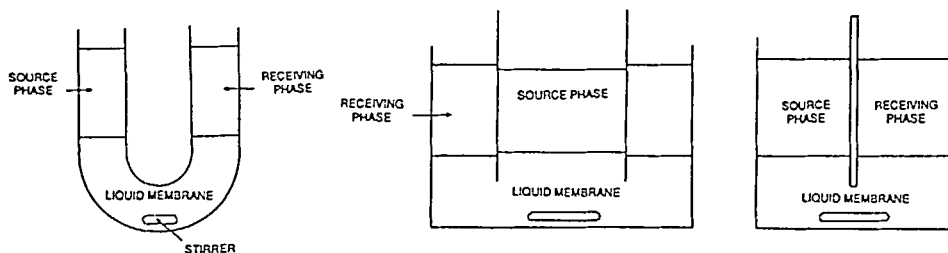


FIGURE 1 Bulk liquid membrane devices. A liquid heavier than water interfaces two aqueous layers. In the three displayed devices, the liquid membrane is magnetically stirred; the aqueous layers can be stirred mechanically.

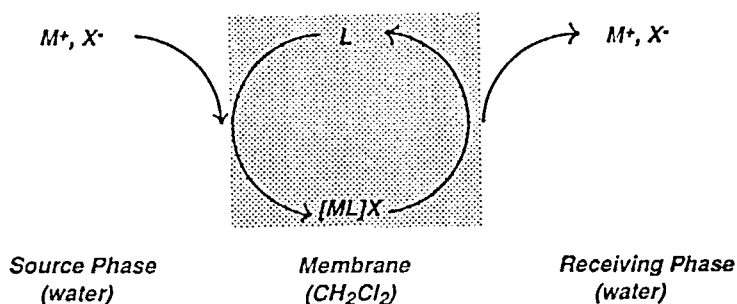


FIGURE 2 Scheme of the transport of an MX salt, across a liquid membrane, mediated by a carrier L. The transport of MX is driven by its concentration gradient.

The most common transport experiment profits from a gradient of concentration. A classical example is given by the transport of a salt MX to a receiving phase which is pure water. The carrier can be a molecule L which presents coordinating properties towards the cation  $M^+$ ;  $M^+$  is extracted by L into the membrane in the form of the metal complex  $[ML]^+$ . To maintain electroneutrality, an  $X^-$  anion is also extracted into the membrane. The  $[ML]X$  ion pair diffuses to the other side of the membrane: here, if the  $[ML]^+$  complex in the water immiscible solvent is not too stable, the MX salt is released to the aqueous receiving layer. The carrier molecule L is now ready for the next trip and it will shuttle indefinitely across the membrane according to the mechanism illustrated in Figure 2.

A steady state will be reached when the concentration of the MX salt in the two aqueous phases will be the same. Most of the work on the transport of metal salts driven by a pure concentration gradient has been done, and is currently being done, on block *s* metal ions. In this case L should be a ligand able to give stable complexes with alkali and alkali-earth metal ions: it is not fortuitous that studies on the transport of metal salts across liquid membranes began to develop immediately after *crown ethers*<sup>2</sup> and *cryptands*<sup>3</sup> were introduced in coordination chemistry. The concepts of selective binding of block *s* metal ions by macrocyclic ligands of varying structural features (ring and cavity size, number of donor atoms *etc.*), developed through single-phase equilibrium studies, were used to design appropriate carriers for selective transport and separation of metal ions.<sup>4</sup> The relationship between the metal-carrier

binding constant and the rate of the transport across the liquid membrane is now clearly defined.<sup>5</sup>

Whereas hundreds of papers have been reported on the selective transport of block *s* metal ions, very few investigations have been devoted to the carrier mediated transport of block *d* metal centres across liquid membranes, driven by a concentration gradient.<sup>6</sup> The main reason of this is that ligands used as carriers form in general too stable complexes with the transition metal ion to be transported and the energy gain associated to the hydration of the ions released to the aqueous receiving phase is not favourable enough to compensate the energy loss associated to the carrier demetallation.

It should be finally mentioned that the general requisite that a molecular system should satisfy, in order to act as a carrier in this type of experiments, is that it should be soluble in the liquid membrane and completely insoluble in water. To obtain this, one can simply append some lipophilic group (*i.e.* a long aliphatic chain) on the chosen system. The site of the lipophilic functionality should be far enough from the binding site to avoid any possible interference.

The limit of the transport experiment driven by the concentration gradient is that the steady state is reached when both source and receiving phases are 50% in MX. Thus, if you are interested to separate or purify a given salt using this method, you should be prepared to loose back in the source phase one half of the object of your interest.

## 2. TAKING ADVANTAGE OF A pH GRADIENT

The transport of the species of interest A can be coupled to the transport of an auxiliary species B, provided that both A and B compete for the same carrier. In these circumstances, if the concentration gradient of the species B is kept in some way constant, 100% transport of A is achieved. Consider for instance the case of a lipophilic system  $L^{n-}$ , which forms a stable complex with a metal ion  $M^{n+}$  and is also a Brönsted base. In this case, the  $H^+$  ion can be used as an auxiliary species. The scheme of such type of transport is illustrated in Figure 3.

The source phase contains  $M^{n+}$ , say in  $10^{-2}$  M concentration, the receiving phase is much more concentrated in  $H^+$ , *e.g.* 1 M. The carrier system carries metal ions in the form of  $[ML]$  and carries protons, in the opposite direction, in the form of  $H_nL$ . When all the  $M^{n+}$  ions have been stripped from the source phase, the concentration gradient for the auxiliary species  $H^+$  has decreased only by a smaller amount (1%, if  $n=1$ , 2% if  $n=2$ , etc.). It is curious that some authors ignore, or choose not to mention, the existence of this substantial gradient and state that the  $M^{n+}$  transport goes on against its concentration gradient (*uphill* transport).

We have used this mechanism to perform specific transport of  $Cu^{2+}$  across a liquid membrane.<sup>7</sup> The  $H_2L$  carrier we used was a lipophilic version of dioxocyclam (1): the ability of the ligand 1 in aqueous solution to incorporate  $Cu^{2+}$  with simultaneous extrusion of two protons from the amide groups has been well documented through equilibrium studies.<sup>8</sup> The process is quickly reversible: in presence of acid, the  $[Cu^{II}\{dioxocyclamato(2-)\}]$  complex decomposes to give  $Cu^{2+}$  and dioxocyclam again. For transport studies, a long aliphatic chain was appended on the ligand's carbon backbone to confine the carrier in the membrane.

In the transport experiment, cetyldioxocyclam (2) was dissolved in the membrane.

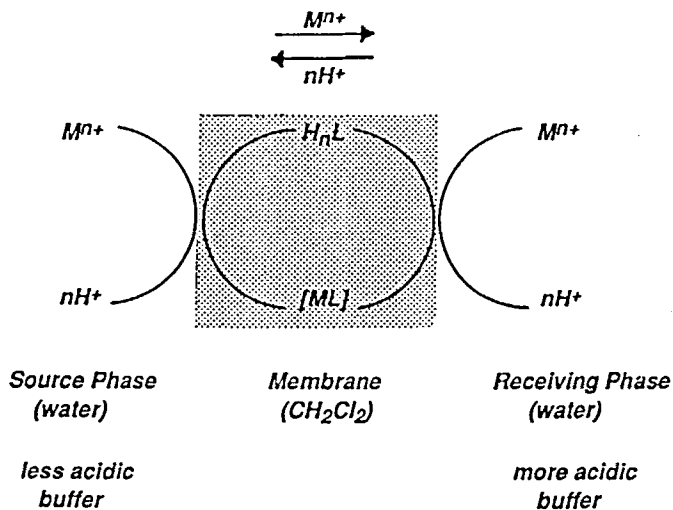
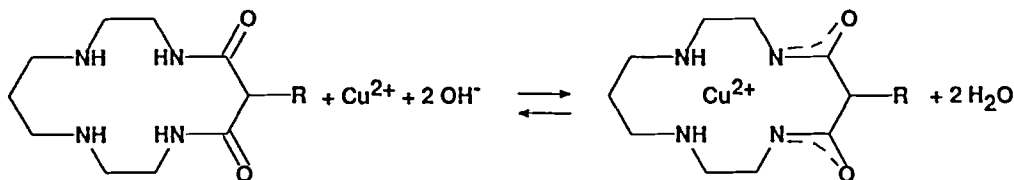


FIGURE 3 Scheme of the transport of an  $M^{n+}$  cation across a liquid membrane mediated by the carrier system  $L^-/H_nL$ . The flow of  $M^{n+}$  is coupled to the counterflow of the auxiliary species  $H^+$ . The cross transport of  $M^{n+}$  and  $nH^+$  cations is driven by a pH gradient.



R = H dioxocyclam 1

R =  $C_{16}H_{33}$  cetyldioxocyclam 2

The  $Cu^{2+}$  source phase was adjusted to  $pH = 7$  using the TRIS buffer (thus, the metal ion was not present as an aquo-ion, but as an amine complex: indeed, the colour of the solution was intense blue). The receiving phase was adjusted to  $pH = 3$  by the phthalate buffer. The concentration of the buffer was 10 times greater than that of copper(II). In the course of the experiment,  $[Cu^{II}L]$  travels across the dichloromethane layer from the aqueous neutral solution to the acidic one.  $H_2L$  does the opposite trip. The scheme of the transport process is outlined in Figure 4. Through this mechanism, it was possible to transport more than 50% of the original copper(II) ions. Noticeably, the rate of the  $Cu^{2+}$  transport is not influenced by the presence of other 3d divalent metal ions:  $Fe^{2+}$ ,  $Co^{2+}$ ,  $Ni^{2+}$  and  $Zn^{2+}$ . This depends upon the fact that most of the above ions do not establish coordinative interactions strong enough to compensate the very endothermic deprotonation of the two amido groups of the dioxocyclam system.  $Ni^{2+}$  ion does, but its incorporation by cetyl dioxocyclam,

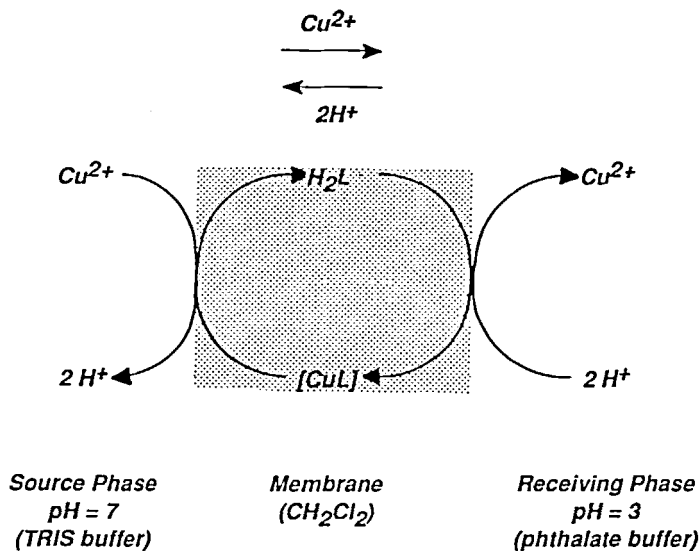


FIGURE 4 pH driven transport of  $\text{Cu}^{2+}$  across a  $\text{CH}_2\text{Cl}_2$  bulk membrane, mediated by cetyldioxocyclam ( $\text{H}_2\text{L}$ ).

**TRANSPORT OF ANIONS DRIVEN BY A pH GRADIENT**  
(co-transport of protons and anions)

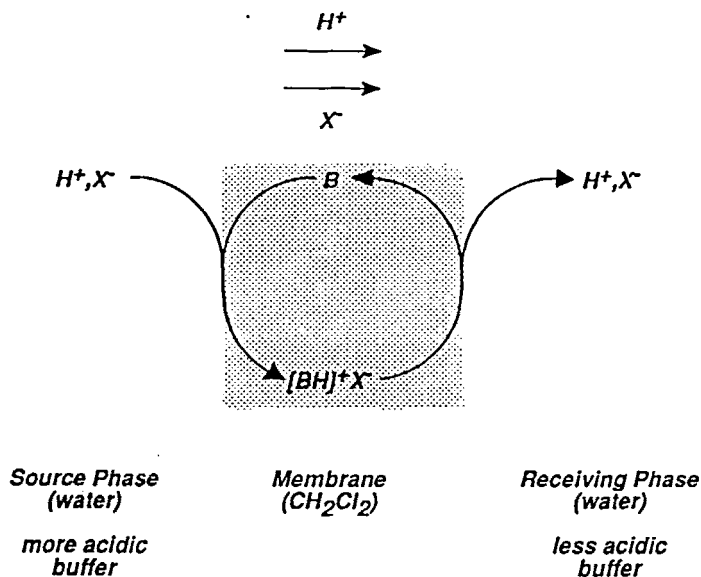


FIGURE 5 Scheme of the transport of an  $\text{X}^-$  anion across a liquid membrane mediated by the carrier system  $\text{B}/[\text{BH}]^+\text{X}^-$ . The flow of  $\text{X}^-$  is coupled to the simultaneous and parallel flow of the auxiliary species  $\text{H}^+$ . The co-transport of  $\text{X}^-$  and  $\text{H}^+$  ions is driven by a pH gradient.

under two-phase conditions, is so slow to prevent any competition with  $\text{Cu}^{2+}$ . Thus, the specificity of  $\text{Cu}^{2+}$  transport derives from a unique combination of thermodynamic and kinetic effects.

It should be noted that using the acid carrier system  $\text{H}_n\text{L}$  and profiting from a pH gradient, only  $\text{M}^{n+}$  ions, and not anions, are transported. Thus, the cation could be recovered from the receiving phase, acidic for the acid  $\text{HX}$ , in the form of  $\text{MX}$  salt.

A pH driven transport can also be performed employing a lipophilic molecular system B, which is a Brönsted base (*e.g.* 1-hexadecylamine). In this case, B will uptake a proton from the acidic aqueous phase; an anion  $\text{X}^-$  will be simultaneously extracted from the same phase, to give the  $[\text{BH}]^+\text{X}^-$  ion pair.  $\text{H}^+$  and  $\text{X}^-$  anions will be released to the basic aqueous phase interface. Therefore, simultaneous transport of protons and anions is observed. Complete stripping of the  $\text{X}^-$  anion from the source phase will be achieved using appropriate acidic and basic buffers.<sup>9</sup> In conclusion, the three-phase pH pump can be used: (i) to separate cations, if the membrane contains an acidic carrier  $\text{H}_n\text{L}$ , (ii) to separate anions, if the membrane contains a basic carrier B.

### 3. TRANSPORT EXPERIMENTS DRIVEN BY A GRADIENT OF REDOX POTENTIAL

Another small particle, other than the proton, can be made to travel across a liquid membrane to drive the transport of a cation  $\text{M}^+$  or of an anion  $\text{X}^-$ : the electron. To make the electron move from an aqueous layer to the other one, we have to create a gradient of redox potential between the two aqueous phases. This can be simply achieved by putting in one of the aqueous layers a reducing agent and in the other one an oxidizing agent. The transport of electrons from the aqueous reducing phase (the Electron Source Phase, ESP) to the aqueous oxidizing phase (the Electron Receiving Phase: ERP) across the membrane has to be carried out by a lipophilic molecular system C, able to display redox activity. Two possibilities are given: (i) the system C is prone to the reduction, to give  $\text{C}^-$ ; (ii) the system C is prone to the oxidation: the cation  $\text{C}^+$  is formed.

Figure 6 describes the three-phase process when the  $\text{C}/\text{C}^-$  redox change operates inside the membrane: C is reduced to  $\text{C}^-$  by the aqueous reducing agent Red at the membrane/ESP interface; to keep electroneutrality, an  $\text{M}^+$  cation is simultaneously uptaken from ESP. The  $\text{M}^+\text{C}^-$  ion pair diffuses to the other side of the membrane: here,  $\text{C}^-$  is oxidized under two-phase conditions by the aqueous oxidizing agent Ox and  $\text{M}^+$  is simultaneously released to ERP. In conclusion, after one turnover one  $\text{M}^+$  cation and one electron have been transported from ESP to ERP.

The process involving the  $\text{C}/\text{C}^+$  redox change is illustrated in Figure 7. C is oxidized to  $\text{C}^+$  by the aqueous oxidizing agent Ox at the membrane/ERP interface and an  $\text{X}^-$  anion is extracted into the water immiscible layer to balance the positive charge: the  $\text{C}^+\text{X}^-$  ion pair diffuses to the membrane/ESP interface, where  $\text{C}^+$  is reduced to C by the aqueous reducing agent Red and  $\text{X}^-$  is released to ESP. For each  $\text{C}/\text{C}^+$  cycle, one anion  $\text{X}^-$  is transported from ERP to ESP and one electron is transported in the opposite direction.

Three-phase systems in which the aqueous layers present a different redox potential can be used to separate cations or anions in a way analogous to three-phase systems based on a pH gradient: the use of a  $\text{C}/\text{C}^-$  carrier system allows the transport and separation of cations  $\text{M}^+$  (as an HL carrier does in the pH pump), the use of the

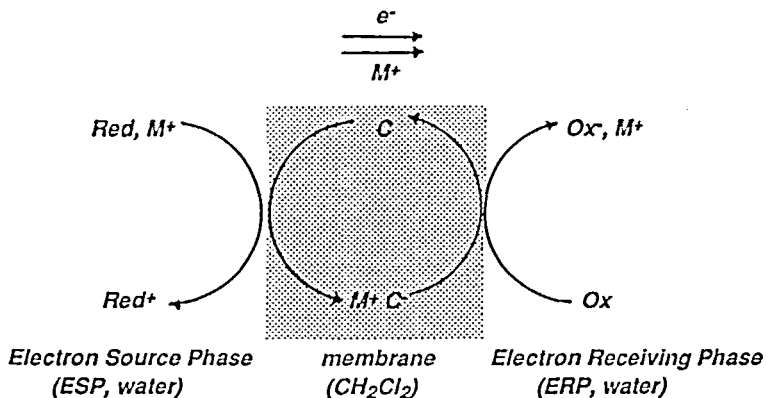


FIGURE 6 Scheme of the transport of an  $\text{M}^+$  cation across a liquid membrane, driven by a gradient of redox potential. A  $\text{C}/\text{C}^-$  redox system operates inside the membrane. The redox system, in its reduced form, transports electrons and cations from the aqueous reducing layer to the aqueous oxidizing layer. A co-transport of  $\text{e}^-$  and  $\text{M}^+$  is observed.

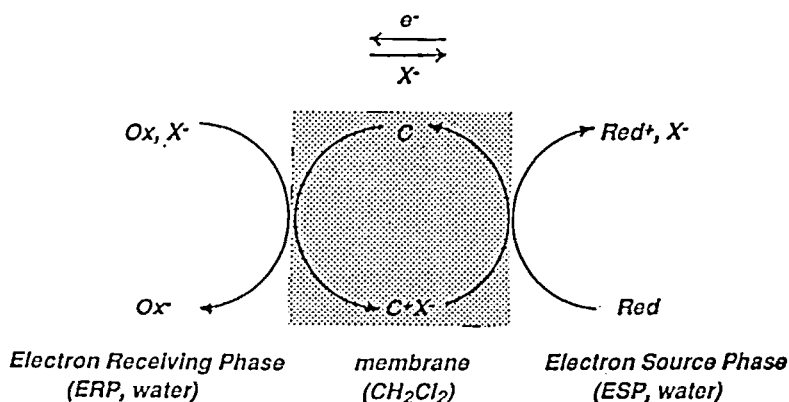
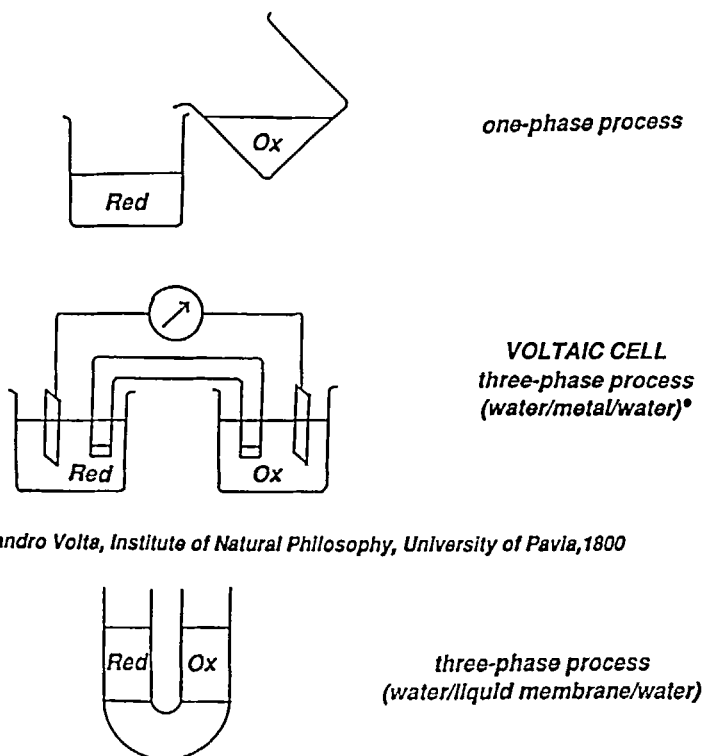


FIGURE 7 Scheme of the transport of an  $\text{X}^-$  anion across a liquid membrane, driven by a gradient of redox potential. A  $\text{C}/\text{C}^+$  redox system operates inside the membrane. The redox system, in its reduced form (C), transports electrons from the aqueous reducing layer to the aqueous oxidizing layer, whereas in its oxidized form ( $\text{C}^+$ ) it transports anions  $\text{X}^-$  in the opposite direction. A cross transport of  $\text{e}^-$  and  $\text{X}^-$  is observed.



$C/C^+$  carrier system allows separation of anions  $X^-$  (in analogy with pH driven experiments in which a carrier B is used). Also in this case, to get 100% transport of the species of interest ( $M^+$  or  $X^-$ ) one should buffer the aqueous layer with an excess of the auxiliary reagents: the oxidizing agent and the reducing agent.

However, we looked at electron transport experiments from a different standpoint. In particular, we were attracted by the possibility to carry out oxidation and reduction reactions in a non-conventional way *i.e.* keeping the solutions of the oxidizing agent and of the reducing agent separated. Indeed, a device to carry out redox processes with separated aqueous reagents has been invented nearly two centuries ago by Alessandro Volta, in our University.<sup>10</sup> As a matter of fact, in the voltaic cell the oxidizing agent and the reducing agent are not in contact. Electrons flow from the reducing half-cell (ESP) to the oxidizing half-cell (ERP) through a metal wire. To keep electroneutrality, ions move across the salt bridge. In the liquid membrane device, electrons flow through the water immiscible layer carried by a molecular system, which behaves as a shuttle; the same carrier is used to transport ions from an aqueous layer to the other. The three ways to perform oxidation and reduction reactions in a single phase (a) or under multi-phase conditions (b and c) are illustrated in Figure 8.



\* *Alessandro Volta, Institute of Natural Philosophy, University of Pavia, 1800*

FIGURE 8 Three possible ways to carry out oxidation and reduction reactions in solution: (a) the classical procedure of mixing a solution of the oxidizing agent and a solution of the reducing agent; (b) through Volta's electrical cell; (c) through the three-phase device, containing a redox active liquid membrane.

It will be demonstrated in the following paragraphs that using the liquid membrane makes it possible to perform oxidation and reduction reactions in a selective way, *i.e.*, for instance, an oxidizing agent will be able to choose among a collection of reducing agents present in the same solution.

#### 4. METAL COMPLEXES AS ELECTRON CARRIERS: THE $[\text{Fe}^{\text{II,III}}(\text{bipy})_3]^{2+,3+}$ SYSTEM

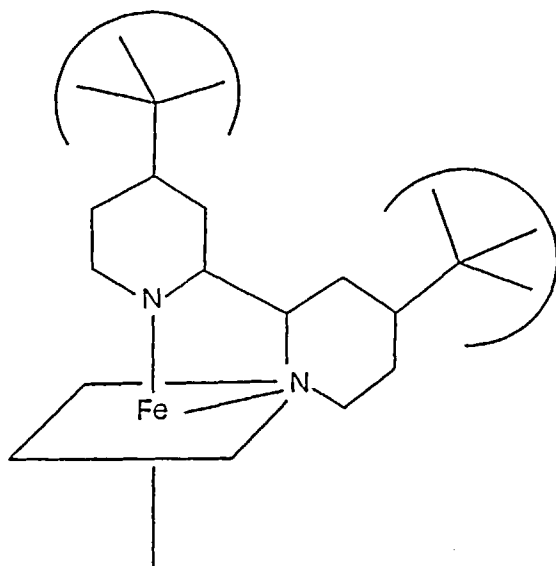
Let us first consider the requirements that a redox system C should satisfy in order to act as a carrier of electrons across a liquid membrane:

- (1) the redox system C has to be confined in the liquid membrane; it has been mentioned in the first paragraph that this general property can be generated on the carrier by introducing on it appropriate lipophilic functionalities;
- (2) the redox change in which C is involved should be fast, reversible and should take place, possibly, according to an uncomplicated one-electron step;
- (3) the potential pertinent to the redox system to be used as a carrier should be intermediate between the potential associated to the aqueous oxidizing agent and that associated to the aqueous reducing agent:  $E_{\text{ox}} > E_c > E_{\text{red}}$ .

The latter statement is not trivial, as one has to compare quantities belonging to the classical electrochemical scale in water,  $E_{\text{ox}}$  and  $E_{\text{red}}$ , to a quantity,  $E_c$ , measured in the water immiscible liquid used as a membrane (*e.g.*  $\text{CH}_2\text{Cl}_2$ ): this comparison can be made only on empirical bases (*vide infra*).

As far as the choice of the electron carrier is concerned, point (2) could suggest to look at redox systems containing a metal centre. One hundred years of coordination chemistry have produced many beautiful metal complexes prone to fast and reversible one-electron redox changes. We decided to begin from one of the most classical systems, *i.e.* complexes of 2,2'-bipyridine (*bipy*). In particular, we started with the  $[\text{Fe}^{\text{II}}(\text{bipy})_3]^{2+}$  complex<sup>11</sup>, which, in water, undergoes a reversible one-electron oxidation process to the  $[\text{Fe}^{\text{III}}(\text{bipy})_3]^{3+}$  species, at the potential of 1.11 V *vs* SHE. However, iron(II) and iron(III) complexes of plain *bipy* cannot work as carriers, as, even if soluble in  $\text{CH}_2\text{Cl}_2$ , they partition between water and dichloromethane. Thus, to satisfy requirement (1), we took a more lipophilic derivative: 4,4'-di-*tert*-butyl-2,2'-bipyridine ( $\text{L}^1$ )<sup>11</sup>. In fact, the corresponding  $[\text{Fe}^{\text{II}}\text{L}_3^1](\text{ClO}_4)_2$  and  $[\text{Fe}^{\text{III}}\text{L}_3^1](\text{ClO}_4)_3$  octahedral complexes, due to the six tertiary butyl groups, present a sort of "greasy skin", which imparts complete insolubility in water.

Cyclic voltammetry experiments in a  $\text{CH}_2\text{Cl}_2$  solution, made 0.1 M in  $\text{Bu}_4\text{NClO}_4$ , indicated that the  $\text{Fe}^{\text{II}}/\text{Fe}^{\text{III}}$  redox change takes place reversibly at 0.55 V (*vs* the internal reference couple ferrocenium/ferrocene,  $\text{Fc}^+/\text{Fc}$ ). Then, the reactivity of the  $\text{Fe}^{\text{II}}$  and  $\text{Fe}^{\text{III}}$  complexes in  $\text{CH}_2\text{Cl}_2$  solution with aqueous redox reagents was investigated through two-phase experiments. In particular, a red  $\text{CH}_2\text{Cl}_2$  layer of the  $[\text{Fe}^{\text{II}}\text{L}_3^1](\text{ClO}_4)_2$  complex, when equilibrated (*i.e.* vigorously shaken) with an aqueous layer containing the quite strong oxidizing agent  $\text{Ce}^{\text{IV}}$  in 1 M  $\text{HClO}_4$  ( $E^\circ = 1.70$  *vs* SHE), takes a green colour, the colour of the  $[\text{Fe}^{\text{III}}\text{L}_3^1](\text{ClO}_4)_3$  complex. On the other hand, if this green layer is equilibrated with an aqueous layer containing the mild reducing agent  $\text{Fe}^{\text{II}}$ , in 1 M  $\text{HClO}_4$ , the red colour forms again, indicating chemical reversibility of the two-phase oxidation and reduction processes. Now, on the basis of the simple experiments described above, we can try



to juxtapose the two electrochemical scales pertinent to this study: the familiar electrochemical scale in water ( $E^\circ$  values *vs* SHE) and the more exotic electrochemical scale in dichloromethane ( $E^\circ$  values *vs*  $Fc^+/Fc$ ). We mentioned before that this juxtaposition can be only empirical. In particular, the two-phase experiment described before suggests that the two scales should be juxtaposed as depicted in Figure 9.

According to Figure 9, the potential associated to the  $[Fe^{III}L_3](ClO_4)_3/[Fe^{II}L_3](ClO_4)_2$  redox couple in  $CH_2Cl_2$  is lower than that associated to the aqueous  $Ce^{IV}/Ce^{III}$  couple (in fact,  $Ce^{IV}$  oxidizes  $[Fe^{II}L_3](ClO_4)_2$ , under two-phase conditions), but higher than that associated to the aqueous  $Fe^{III}/Fe^{II}$  couple ( $Fe^{II}$  reduces  $[Fe^{III}L_3](ClO_4)_3$ , under two-phase conditions). If the juxtaposition of Figure 9 is correct, it should happen that the green  $[Fe^{II}L_2](ClO_4)_2$  complex should be reduced, under two-phase conditions, by every aqueous reducing agent whose potential is lower than that associated to the  $Fe^{III}/Fe^{II}$  couple. Thus, several conventional aqueous reducing agents, of different nature and power, were tested:  $[Fe^{II}(CN)_6]^{4-}$ ,  $NO_2^-$ ,  $SO_3^{2-}$ , all exhibiting a lower potential than  $Fe^{II}$  (see Figure 9). Indeed, all of them make the green  $CH_2Cl_2$  layer turn red, on shaking.

The diagram in Figure 9 fully illustrates the thermodynamic aspects of the reduction of  $[Fe^{III}L_3](ClO_4)_3$  under two-phase conditions. We were also interested to look at the kinetic aspects of this two-phase process. In this connection, we designed the following experiment: in a 1 cm quartz cuvette 2.0 cm<sup>3</sup> of a  $CH_2Cl_2$  solution  $5 \times 10^{-4} M$  in  $[Fe^{III}L_3](ClO_4)_3$  and 1.0 cm<sup>3</sup> of an aqueous solution 0.1 N in one of the previously mentioned reducing agents ( $Fe^{2+}$ ,  $[Fe^{II}(CN)_6]^{4-}$ ,  $NO_2^-$ ,  $SO_3^{2-}$ ) were carefully stratified. Spectra in the UV-vis region of the  $CH_2Cl_2$  layer, magnetically stirred at a constant rate, were taken at selected time intervals. The progress of the two-phase redox process was monitored through the intensity of the bands pertinent to the red  $[Fe^{II}L_3](ClO_4)_2$  species, which forms on reduction. The variation with the time

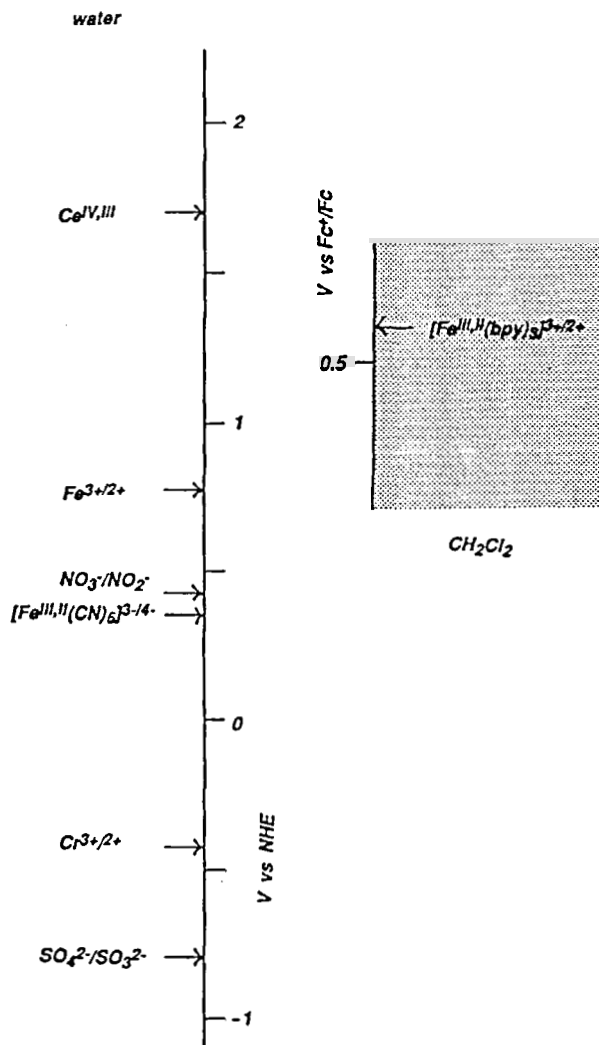
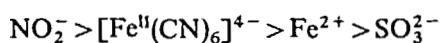


FIGURE 9 Juxtaposition of the electrochemical scale in water ( $V$  vs SHE) and of the electrochemical scale in  $\text{CH}_2\text{Cl}_2$  ( $V$  vs  $\text{Fc}^+/\text{Fc}$ ), as derived from two-phase redox experiments on the  $[\text{Fe}^{\text{II,III}}\text{L}_3](\text{ClO}_4)_3/[\text{Fe}^{\text{II}}\text{L}_3](\text{ClO}_4)_2$  couple.

of the concentration of the  $\text{Fe}^{\text{II}}$  complex in the  $\text{CH}_2\text{Cl}_2$  layer in the course of the experiments with the investigated reducing agents is plotted in the diagram of Figure 10.

The slope of the linear part of each concentration profile expresses the rate of the two-phase process in the conditions of the experiment (in the spectrophotometric cuvette). Rates decrease according to the following sequence:



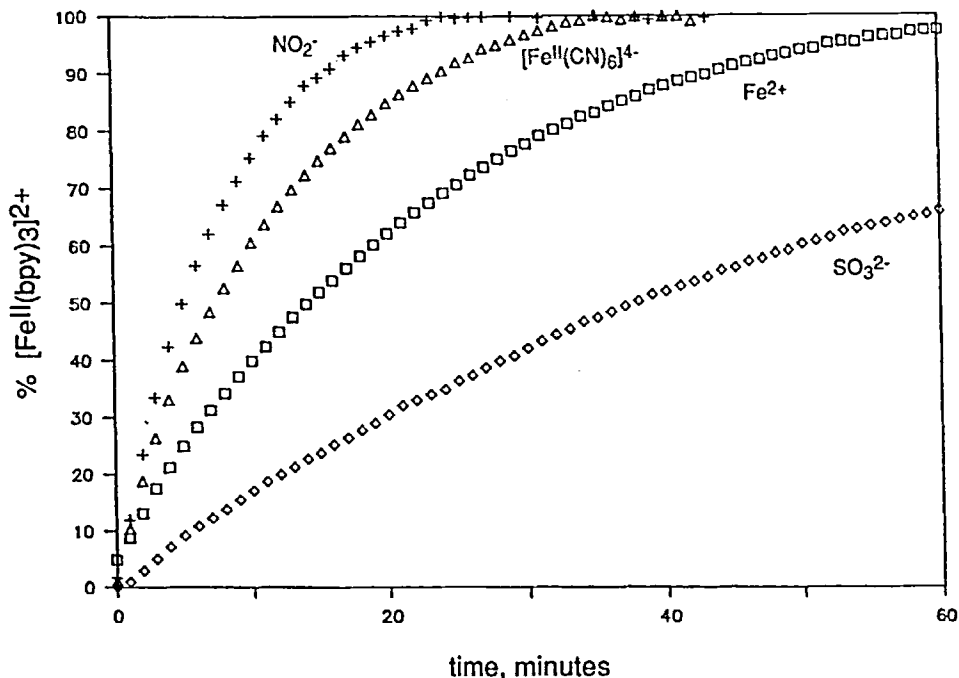


FIGURE 10 Two-phase reduction of  $[\text{Fe}^{\text{III}}\text{L}_3](\text{ClO}_4)_3$  by aqueous reducing agents. Concentration profiles of the  $[\text{Fe}^{\text{III}}\text{L}_3](\text{ClO}_4)_3$  species in the  $\text{CH}_2\text{Cl}_2$  layer, inside a spectrophotometric cuvette (see text).

The above sequence should reflect the sequence of the rate of the electron transfer process between the reducing agent and the  $[\text{Fe}^{\text{II}}\text{L}_3](\text{ClO}_4)_3$  complex at the water/dichloromethane interface, *i.e.* in that boundary region in which  $\text{H}_2\text{O}$  and  $\text{CH}_2\text{Cl}_2$  molecules mix together. Tris-bipyridine complexes are typical outer-sphere redox agents. The order of the rates of the two-phase reduction of  $[\text{Fe}^{\text{III}}\text{L}_3](\text{ClO}_4)_3$  by  $[\text{Fe}^{\text{II}}(\text{CN})_6]^{4-}$  and  $\text{Fe}^{2+}$  parallels the order of the self-exchange constants of the aqueous reducing agents ( $[\text{Fe}^{\text{II}}(\text{CN})_6]^{4-}$ ,  $k_{11} = 7.4 \times 10^2 \text{ M}^{-1} \text{ s}^{-1}$ ;  $\text{Fe}^{2+}$ ,  $k_{11} = 4 \text{ M}^{-1} \text{ s}^{-1}$ ). The reducing power of the aqueous reagents employed does not seem directly related to the rate sequence: in particular, the strongest aqueous reducing agent ( $\text{SO}_3^{2-}$ ,  $E^\circ = -0.70 \text{ V vs SHE}$ , at  $\text{pH} = 10$ ) gives the slowest two-phase reduction. Transport (three-phase) experiments were performed using the glass cell shown in Figure 11. In the V-shaped tube a layer of  $\text{CH}_2\text{Cl}_2$  (the liquid membrane, volume:  $30 \text{ cm}^3$ ) separates two  $30 \text{ cm}^3$  aqueous layers. In a typical experiment, the membrane was made  $5 \times 10^{-4} \text{ M}$  in  $[\text{Fe}^{\text{II}}\text{L}_3](\text{ClO}_4)_2$ , the aqueous oxidizing layer (ERP) was  $0.1 \text{ M}$  in  $\text{Ce}^{\text{IV}}$ , the aqueous reducing layer (ESP) was  $10^{-2} \text{ M}$  in  $\text{Fe}^{\text{II}}$  or  $[\text{Fe}^{\text{II}}(\text{CN})_6]^{4-}$ . The liquid membrane was magnetically stirred at 200 rpm, each aqueous layer was stirred by a glass rod driven by a synchronous motor, rotating at a constant rate (200 rpm).

Occurrence and progress of the transport of electrons from ESP to ERP was monitored by taking the spectra of portions of the aqueous reducing solutions, which were syringed out at selected time intervals. In particular, the intensity of the

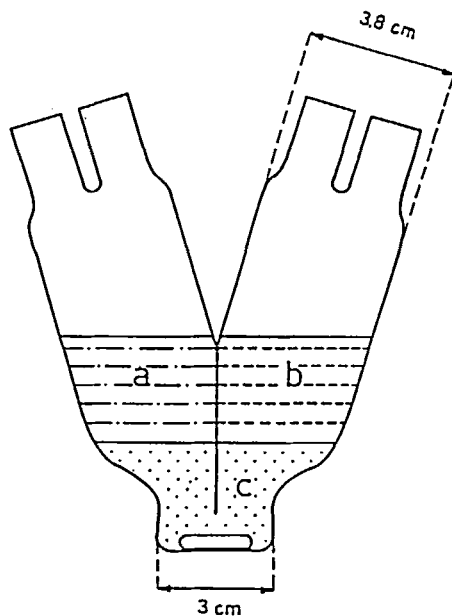


FIGURE 11 V-shaped glass cell used for the electron transport experiments. The two aqueous layers ( $30\text{ cm}^3$  each) are separated by a glass wall and by an interfacing layer of  $\text{CH}_2\text{Cl}_2$  (the liquid membrane,  $30\text{ cm}^3$ ).

absorption bands pertinent to the oxidized form of the aqueous reducing agent ( $\text{Fe}^{\text{III}}$  and  $[\text{Fe}^{\text{III}}(\text{CN})_6]^{3-}$ , respectively) were considered. Figure 12 shows the corresponding transport profiles.

Figure 13 illustrates the general transport scheme for the two experiments. The reduced form of the carrier,  $[\text{Fe}^{\text{II}}\text{L}_3](\text{ClO}_4)_2$ , is oxidized by  $\text{Ce}^{\text{IV}}$  at the ERP/membrane interface. A  $\text{ClO}_4^-$  anion is simultaneously extracted from ERP into the membrane to neutralize the positive charge which is formed on the carrier. Thus, the oxidized form of the carrier,  $[\text{Fe}^{\text{III}}\text{L}_3](\text{ClO}_4)_3$ , diffuses to the other side of the membrane. Here, it is reduced by the aqueous reducing agent,  $\text{Fe}^{\text{II}}$  or  $[\text{Fe}^{\text{II}}(\text{CN})_6]^{4-}$ ; at the same time, a  $\text{ClO}_4^-$  ion is released to ESP. Notice that the redox system employed is of the  $\text{C}/\text{C}^+$  type and the three-phase experiment involves the cross transport of electrons and of perchlorate anions.

Transport profiles shown in Figure 12 indicate that the rate of the electron transport varies substantially with the nature of the reducing agent: the transport rate, expressed by the slope of the linear part of the  $[\text{Red}^+]$  concentration *vs* time curve, is considerably higher (nearly twice) for  $[\text{Fe}^{\text{II}}(\text{CN})_6]^{4-}$  than for  $\text{Fe}^{\text{II}}$ . Notice that this order parallels the sequence observed in two-phase experiments carried out in the spectrophotometric cuvette. Moreover, the fact that the electron transport rate changes with the reducing agent indicates that, in the chosen experimental conditions, the rate determining step of the overall three-phase process takes place at the membrane/ESP interface. However, the rate determining step can be moved to the other side of the membrane by changing the relative concentrations of the aqueous redox agents in ESP and ERP. We carried out a new series of experiments, in which

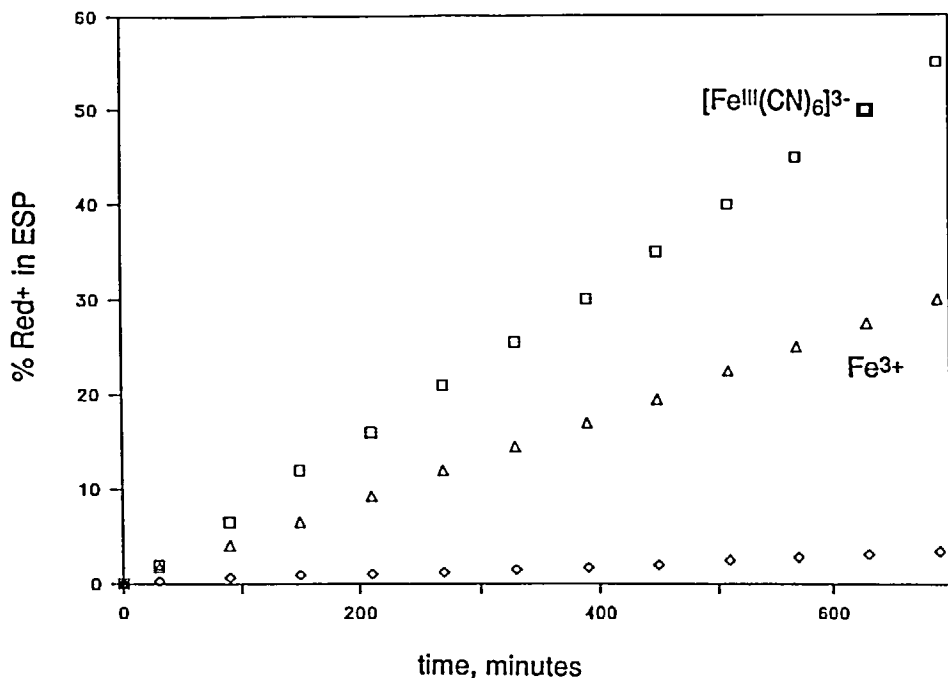


FIGURE 12 Transport profiles for a  $\text{Ce}^{\text{IV}}/[\text{Fe}^{\text{II}}\text{L}_3](\text{ClO}_4)_2/[\text{Fe}^{\text{III}}\text{L}_3](\text{ClO}_4)_3/\text{Fe}^{\text{II}}$  (or  $[\text{Fe}^{\text{II}}(\text{CN})_6]^{4-}$ ) experiment. The limiting reagent is  $\text{Fe}^{\text{II}}$  (or  $[\text{Fe}^{\text{II}}(\text{CN})_6]^{4-}$ ) and the progress of the three-phase redox process is monitored through the variation of the concentration of the oxidized form of the aqueous reducing agent:  $\text{Fe}^{\text{III}}$  (or  $[\text{Fe}^{\text{III}}(\text{CN})_6]^{3-}$ ).

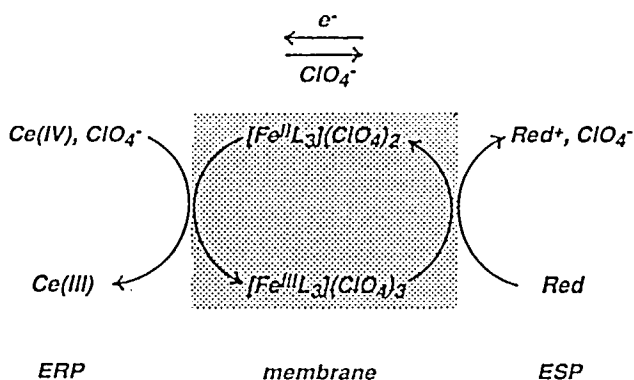


FIGURE 13 Transport scheme for experiments involving the  $[\text{Fe}^{\text{II}}\text{L}_3](\text{ClO}_4)_2/[\text{Fe}^{\text{III}}\text{L}_3](\text{ClO}_4)_3$  redox system as a carrier. The redox system belongs to the C/C<sup>+</sup> type and the transport of electrons is coupled to the countertransport of anions  $\text{X}^-$  in the opposite direction ( $\text{X} = \text{ClO}_4$ ).

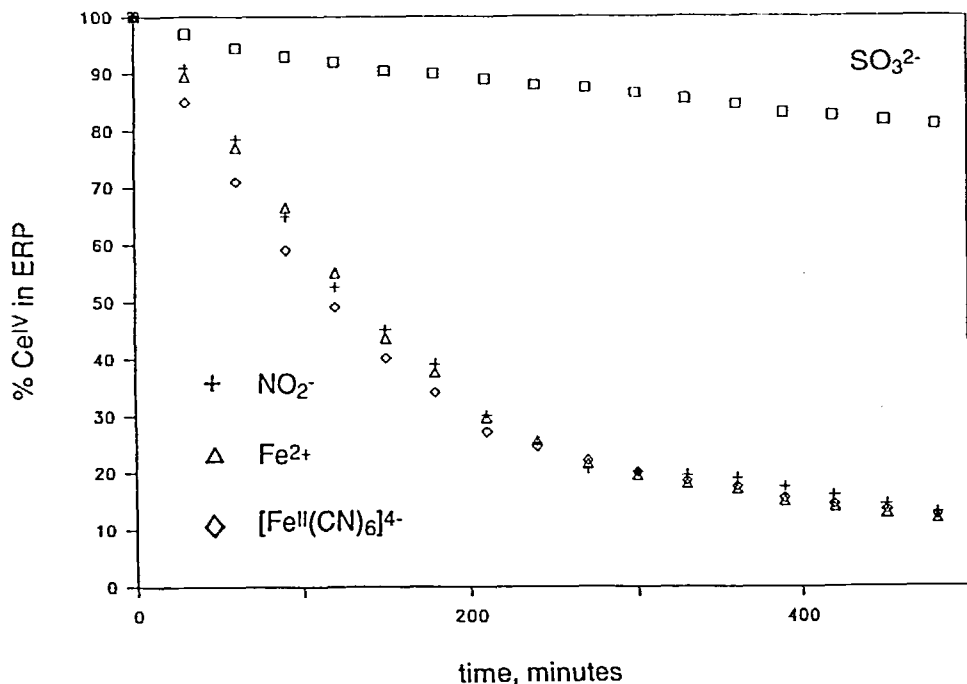


FIGURE 14 Transport profiles for a  $\text{Ce}^{\text{IV}}/[\text{Fe}^{\text{II}}\text{L}_3^1](\text{ClO}_4)_2/[\text{Fe}^{\text{III}}\text{L}_3^1](\text{ClO}_4)_3/\text{Red}$  experiment (Red =  $\text{Fe}^{\text{II}}$ ,  $[\text{Fe}^{\text{II}}(\text{CN})_6]^{4-}$ ,  $\text{NO}_2^-$ ,  $\text{SO}_3^{2-}$ ). The limiting reagent is  $\text{Ce}^{\text{IV}}$  and the progress of the three-phase redox process is monitored through the variation of its concentration.

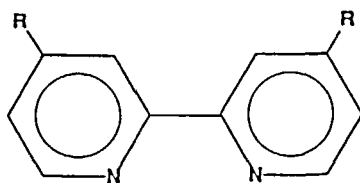
$\text{Ce}^{\text{IV}}$  was the limiting reagent, being  $10^{-2}$  M, whereas the reducing agent in ESP was in excess concentration:  $10^{-1}$  M. Progress of the electron transport was monitored through the decrease, spectrophotometrically measured, of the concentration of  $\text{Ce}^{\text{IV}}$  in ERP. Corresponding transport profiles are shown in Figure 14.

It is now seen that the transport rate is the same for both  $\text{Fe}^{\text{II}}$  and  $[\text{Fe}^{\text{II}}(\text{CN})_6]^{4-}$  (and even for the  $\text{NO}_2^-$  anion). The different nature of the reducing agent cannot affect the overall transport rate, as the sluggish step, due to a concentration effect, takes place at the ERP/membrane interface. Selective, and particularly slow, electron transport is observed only with the  $\text{SO}_3^{2-}$  ion. This should be ascribed to the fact that the rate of the two-phase reduction of  $[\text{Fe}^{\text{III}}\text{L}_3^1](\text{ClO}_4)_3$  by  $\text{SO}_3^{2-}$  is so intrinsically low (as also indicated by the preliminary experiments in the spectrophotometric cuvette, *vide supra*) to more than compensate the favourable concentration effect.

## 5. HOW LIPOPHILIC SHOULD THE CARRIER BE

The chosen redox system has to be confined inside the membrane, as required by the first of the principles to be followed in the design of an electron carrier. In the example illustrated in the previous paragraph, appending of six tertiary butyl groups on the tris-bipyridine framework prevented both reduced ( $\text{Fe}^{\text{II}}$ ) and oxidized ( $\text{Fe}^{\text{III}}$ )





R = H                      bipy

R = C(CH<sub>3</sub>)<sub>3</sub>              L<sup>1</sup>

R =  $\begin{array}{c} \text{(CH}_2\text{)}_3\text{CH}_3 \\ | \\ \text{CH} \\ | \\ \text{(CH}_2\text{)}_3\text{CH}_3 \end{array}$               L<sup>2</sup>

forms of the carrier from partitioning between the membrane and the aqueous phases. The question is whether the nature and size of the appended aliphatic group are unimportant or affect the transport properties of the carrier.

In this connection, we synthesized the alkyl substituted bipyridine: (L<sup>2</sup>, 4,4'-di-(1-butylpentyl)-2,2'-bipyridine) and we compared the transport properties of the corresponding Fe<sup>II</sup> complex, [Fe<sup>II</sup>L<sub>3</sub><sup>1</sup>](ClO<sub>4</sub>)<sub>2</sub>, with those of the 4,4'-di-*tert*-butyl-2,2'-bipyridine complex, [Fe<sup>II</sup>L<sub>3</sub><sup>1</sup>](ClO<sub>4</sub>)<sub>2</sub>. First, we carried out two-phase oxidation processes in a cuvette, in which 2.0 cm<sup>3</sup> of a CH<sub>2</sub>Cl<sub>2</sub> solution 5 × 10<sup>-4</sup> M in [Fe<sup>II</sup>L<sub>3</sub><sup>1</sup>](ClO<sub>4</sub>)<sub>2</sub> or in [Fe<sup>II</sup>L<sub>3</sub><sup>2</sup>](ClO<sub>4</sub>)<sub>2</sub> and 1.0 cm<sup>3</sup> of an aqueous solution 0.1 M in Ce<sup>IV</sup> were stratified. Photons were allowed to cross the magnetically stirred CH<sub>2</sub>Cl<sub>2</sub> layer and the progress of the two-phase reaction was followed through the decay of the absorption bands pertinent to the Fe<sup>II</sup> chromophore. The decrease with the time of the concentration of the Fe<sup>II</sup> complexes with the two bipyridines of different lipophilicity dissolved in the CH<sub>2</sub>Cl<sub>2</sub> layer is shown in Figure 15. Figure 15 shows that the rate of the two-phase oxidation by Ce<sup>IV</sup> is much greater for the [Fe<sup>II</sup>L<sub>3</sub><sup>1</sup>](ClO<sub>4</sub>)<sub>2</sub> species than for the [Fe<sup>II</sup>L<sub>3</sub><sup>2</sup>](ClO<sub>4</sub>)<sub>2</sub> complex. A similar behaviour was observed by studying the two-phase reduction of the oxidized lipophilic complexes [Fe<sup>III</sup>L<sub>3</sub><sup>1</sup>](ClO<sub>4</sub>)<sub>3</sub> and [Fe<sup>III</sup>L<sub>3</sub><sup>2</sup>](ClO<sub>4</sub>)<sub>3</sub> by aqueous Fe<sup>II</sup> in HClO<sub>4</sub>. Figure 16 displays the time dependent increase of the concentration of the lipophilic Fe<sup>II</sup> tris-bipyridine complex, when a 2.0 cm<sup>3</sup> layer 5 × 10<sup>-4</sup> M in [Fe<sup>III</sup>L<sub>3</sub><sup>1</sup>](ClO<sub>4</sub>)<sub>3</sub> or in [Fe<sup>III</sup>L<sub>3</sub><sup>2</sup>](ClO<sub>4</sub>)<sub>3</sub> is equilibrated, through constant rate stirring, with a 1.0 cm<sup>3</sup> aqueous layer 0.1 M in Fe<sup>II</sup> and 1 M in HClO<sub>4</sub>. Also in this case, the two-phase redox process involving the metal complex with the less heavily substituted bipyridine ligand is substantially faster.

Two main reasons can be brought forward to explain this behaviour: (i) the bulkier complex [Fe<sup>II</sup>L<sub>3</sub><sup>2</sup>](ClO<sub>4</sub>)<sub>2</sub> diffuses at a slower rate than the less substituted *bipy* complex [Fe<sup>II</sup>L<sub>3</sub><sup>1</sup>](ClO<sub>4</sub>)<sub>2</sub>; (ii) the thicker "greasy skin" makes more difficult the interaction of the [Fe<sup>II</sup>L<sub>3</sub><sup>2</sup>](ClO<sub>4</sub>)<sub>2</sub> species with aqueous Ce<sup>IV</sup> ion at the membrane/water interface. To verify hypothesis (i), we measured the diffusion coefficients of iron(II) tris-bipyridine complexes in CH<sub>2</sub>Cl<sub>2</sub> solution, using an electrochemical method. In particular, chronoamperometric investigations were carried out, using a

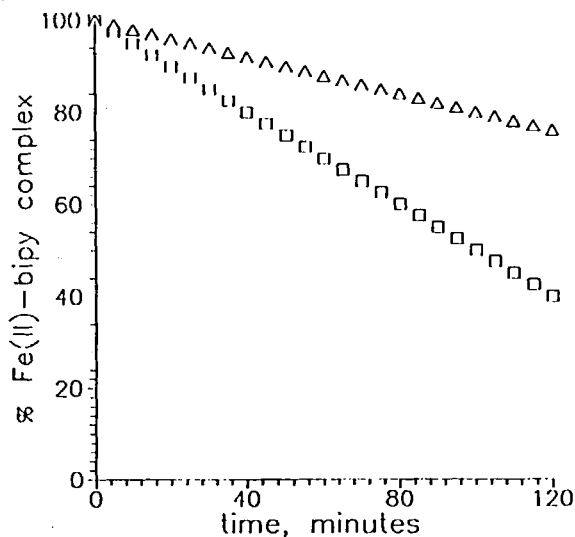


FIGURE 15 Two-phase oxidation (inside the spectrophotometric cuvette) by aqueous  $\text{Ce}^{\text{IV}}$  of two  $[\text{Fe}^{\text{II}}(\text{bipyridine})_3](\text{ClO}_4)_2$  complexes of varying lipophilicity. Bipyridine = 4,4'-di-*tert*-butyl-2,2'-bipyridine ( $L^1$ , □) or 4,4'-di-(1-butylpentyl)-2,2'-bipyridine ( $L^2$ , Δ). Progress of the process is monitored through the decrease with the time of the concentration of the  $\text{Fe}^{\text{II}}$  tris-bipyridine complex in the magnetically stirred  $\text{CH}_2\text{Cl}_2$  layer.

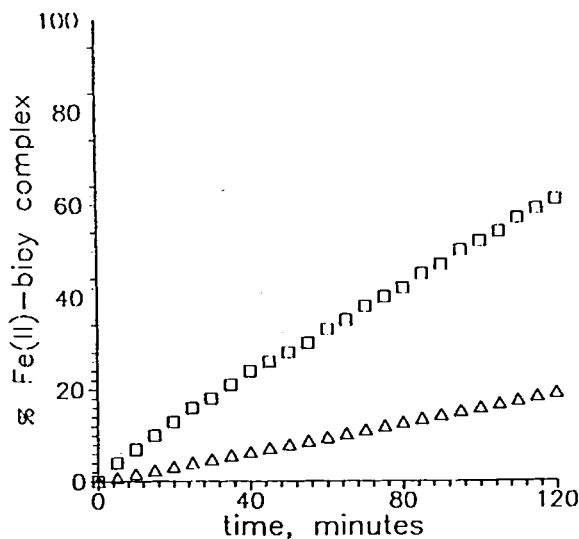


FIGURE 16 Two-phase reduction (inside the spectrophotometric cuvette) by aqueous  $\text{Fe}^{\text{II}}$  of two  $[\text{Fe}^{\text{III}}(\text{bipyridine})_3](\text{ClO}_4)_3$  complexes of varying lipophilicity. Bipyridine = 4,4'-di-*tert*-butyl-2,2'-bipyridine ( $L^1$ , □) or 4,4'-di-(1-butylpentyl)-2,2'-bipyridine ( $L^2$ , Δ). Progress of the process is monitored through the increase with the time of the concentration of the  $\text{Fe}^{\text{II}}$  tris-bipyridine complex in the magnetically stirred  $\text{CH}_2\text{Cl}_2$  layer.

spherical platinum electrode, on  $\text{CH}_2\text{Cl}_2$  solutions 0.1 M in  $\text{Bu}_4\text{NClO}_4$  and  $10^{-3}$  M in the  $[\text{Fe}^{\text{II}}(\text{bipyridine})_3](\text{ClO}_4)_2$  complex, at  $25^\circ\text{C}$ . In addition to the previously discussed complexes with  $\text{L}^1$  and  $\text{L}^2$ , the complex with the parent ligand *bipy* was considered.

Diffusion coefficients  $D$  ( $\text{cm}^2\text{s}^{-1}$ ), calculated from the Cottrell equation, are:  $[\text{Fe}^{\text{II}}(\text{bipy})_3](\text{ClO}_4)_2$ ,  $3.24 \times 10^{-6}$ ;  $[\text{Fe}^{\text{II}}\text{L}_3^1](\text{ClO}_4)_2$ ,  $3.81 \times 10^{-6}$ ;  $[\text{Fe}^{\text{II}}\text{L}_3^2](\text{ClO}_4)_2$ ,  $4.74 \times 10^{-6}$ .<sup>12</sup> The above data indicate that increasing bulkiness of the tris-bipyridine complex does not hinder its diffusion in the  $\text{CH}_2\text{Cl}_2$  solution, but, on the contrary, makes it slightly easier. Thus, the sluggishness of the two-phase oxidation of  $[\text{Fe}^{\text{II}}\text{L}_3^2](\text{ClO}_4)_2$  should be rather ascribed to factor (ii), i.e. to the difficult approach and interaction of the carrier with the aqueous reactant, due to its more pronounced lipophilicity.

For a further comparison, electron transport experiments of the type previously described were carried out, using the  $[\text{Fe}^{\text{II}}\text{L}_3^2](\text{ClO}_4)_2$  complex as a carrier. The transport was extremely slow and, in particular, the variation of the  $\text{Ce}^{\text{IV}}$  concentration in ERP or of the aqueous reducing agent in ESP after several hours was confined within a few units percent, which corresponds to the experimental uncertainty.

The above results would suggest synthetic chemists, interested in the design of efficient electron carriers, to append on the chosen redox system groups of controlled lipophilicity. In particular, the appended functionalities should present only the minimum lipophilicity and bulkiness required to keep the carrier inside the liquid membrane.

## 6. TRYING TO USE LIGHT TO DRIVE THE ELECTRON TRANSPORT

Another redox couple which can be controlled through coordination by *bipy* is  $\text{Cu}^{\text{II}}/\text{Cu}^{\text{I}}$ . It is well known that 1:2 complexes of  $\text{Cu}^{\text{II}}$  with bipyridines (including phenanthroline) are easily reduced in solution to 1:2 complexes of  $\text{Cu}^{\text{I}}$ . X-ray investigations have demonstrated that the one-electron process involves a drastic stereochemical change. The  $\text{Cu}^{\text{II}}$  complex is five-coordinated, the fifth coordination site of the distorted trigonal bipyramid being occupied by an anion<sup>13</sup>: the  $[\text{Cu}^{\text{II}}(\text{bipy})_2\text{X}]^+$  species exhibits a blue colour. On the other hand, the brick red  $[\text{Cu}^{\text{I}}(\text{bipy})_2]^+$  complex presents a regular tetrahedral stereochemistry.<sup>14</sup> We first studied the reduction of the copper(II) complex of 4,4'-di-*tert*-butyl-2,2'-bipyridine ( $\text{L}^1$ ), under two-phase conditions, using  $\text{Cr}^{\text{II}}$  as a reducing agent. In fact, when equilibrated with an aqueous layer 0.1 M in  $\text{Cr}^{\text{II}}$  and 1 M in  $\text{HCl}$ , the blue  $\text{CH}_2\text{Cl}_2$  layer of the  $[\text{Cu}^{\text{II}}\text{L}_2^1\text{Cl}]\text{Cl}$  complex takes an intense brick red colour, due to the formation of the  $[\text{Cu}^{\text{I}}\text{L}_2^1]\text{Cl}$  chromophore. Kinetic aspects of this two-phase redox process can be investigated in the usual way, inside the spectrophotometric cuvette. Figure 17 shows the variation of the absorption spectrum of the stirred  $\text{CH}_2\text{Cl}_2$  layer: the decrease of the band at 700 nm, assigned to the  $\text{Cu}^{\text{II}}$  complex, is accompanied by the simultaneous increase of the band at 440 nm, which corresponds to the  $\text{Cu}^{\text{I}}$  species.

The potential associated to the  $[\text{Cu}^{\text{II}}\text{L}_2^1\text{Cl}]\text{Cl}/[\text{Cu}^{\text{I}}\text{L}_2^1]\text{Cl}$  couple, measured in  $\text{CH}_2\text{Cl}_2$  solution, 0.1 M in  $\text{Bu}_4\text{NCl}$ , by voltammetric techniques, is  $-0.28$  V vs  $\text{Fc}^+/\text{Fc}$ .

We found convenient to consider the  $[\text{Cu}^{\text{II}}\text{L}_2^1\text{X}]\text{X}/[\text{Cu}^{\text{I}}\text{L}_2^1]\text{X}$  redox change to design two- and three-phase experiments in which light could play some role. In particular,

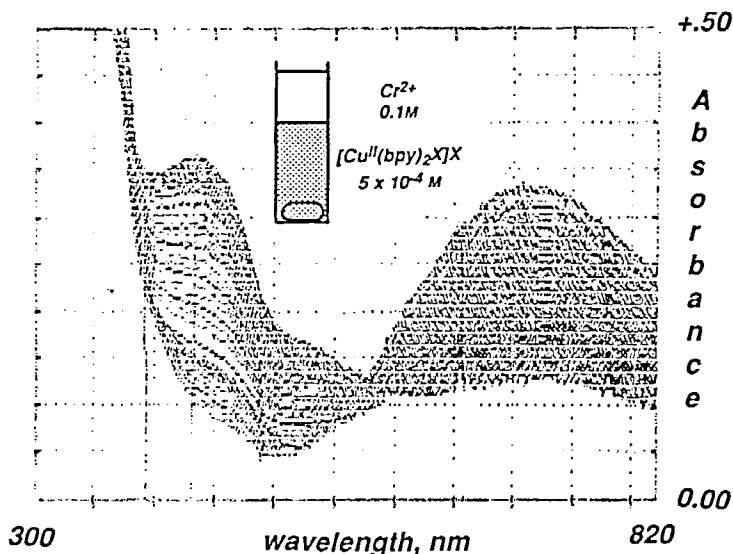


FIGURE 17 Two-phase reduction (inside the spectrophotometric cuvette) of  $[\text{Cu}^{\text{II}}(\text{bipyridine})_2\text{Cl}]\text{Cl}$  by aqueous  $\text{Cr}^{\text{II}}$ . Progress of the experiment is monitored through the decrease of the intensity of the band at 700 nm (pertinent to the blue five-coordinate  $[\text{Cu}^{\text{II}}(\text{bipyridine})\text{Cl}]\text{Cl}$  chromophore) and through the increase of the band at 440 nm (pertinent to the brick red tetrahedral  $[\text{Cu}^{\text{II}}(\text{bipyridine})_2]\text{Cl}$  chromophore).

we carried out the following experiment: in a test tube containing  $3\text{ cm}^3$  of a  $\text{CH}_2\text{Cl}_2$  solution  $5 \times 10^{-4}\text{ M}$  in  $[\text{Cu}^{\text{II}}\text{L}_2\text{Cl}]\text{Cl}$ ,  $3\text{ cm}^3$  of an aqueous solution was stratified: the aqueous layer was  $10^{-2}\text{ M}$  in  $[\text{Co}^{\text{III}}(\text{diamsar})]^{3+}$ ,<sup>15</sup>  $10^{-3}\text{ M}$  in  $[\text{Ru}^{\text{II}}(\text{bipy})_2(\text{bipyC}_2\text{O}_4)]$ ,<sup>16</sup>  $0.1\text{ M}$  in EDTA,  $1\text{ M}$  in NaCl and was adjusted to  $\text{pH}=5$  by a buffer. The two immiscible layers were equilibrated by bubbling dinitrogen in the bottom of the tube. Details of the experiments are pictorially summarized in Figure 18.

In the typical conditions of illumination of the laboratory, no colour changes were observed in the two-phase system. Then, the test tube was illuminated by the halogen lamp of a slide projector, put at a 5 cm distance. The blue non-aqueous layer changes first to green, to take, after a couple of minutes, a definitive brick red colour. The  $\text{CH}_2\text{Cl}_2$  solution was transferred in a quartz cuvette and its spectrum was measured: the spectrum was that of the  $[\text{Cu}^{\text{I}}\text{L}_2]\text{X}$  chromophore. Thus, light promoted, or light triggered, two-phase reduction of  $[\text{Cu}^{\text{II}}\text{L}_2\text{X}]\text{X}$  to  $[\text{Cu}^{\text{I}}\text{L}_2]\text{X}$  has taken place.

The proposed mechanism of the two-phase process is outlined in Figure 19. Through irradiation by visible light, the long living excited state  $[\text{*Ru}^{\text{II}}(\text{bipy})_2(\text{bipyC}_2\text{O}_4)]$  is formed.<sup>17</sup> It is a very strong reducing agent and reduces the  $[\text{Co}^{\text{III}}(\text{diamsar})]^{3+}$  complex to the corresponding  $\text{Co}^{\text{II}}$  species. On the other hand, excess EDTA reduces the  $[\text{Ru}^{\text{II}}(\text{bipy})_2(\text{bipyC}_2\text{O}_4)]^+$  complex which is formed, preventing from back electron transfer and making it ready for a further cycle. The  $[\text{Co}^{\text{II}}(\text{diamsar})]^{2+}$  complex, at the water/dichloromethane interface, reduces  $[\text{Cu}^{\text{II}}\text{L}_2\text{X}]\text{X}$  to  $[\text{Cu}^{\text{I}}\text{L}_2]\text{X}$  (an  $\text{X}^-$  anion should be simultaneously released to water). Using the language of photochemistry, EDTA,  $[\text{*Ru}^{\text{II}}(\text{bipy})_2(\text{bipyC}_2\text{O}_4)]$  and  $[\text{Co}^{\text{III}}(\text{diamsar})]^{3+}$  should be defined, respectively, the sacrificial electron donor, the photosensitizer and the electron relay. Similar systems have been used, for instance, to generate dihydrogen

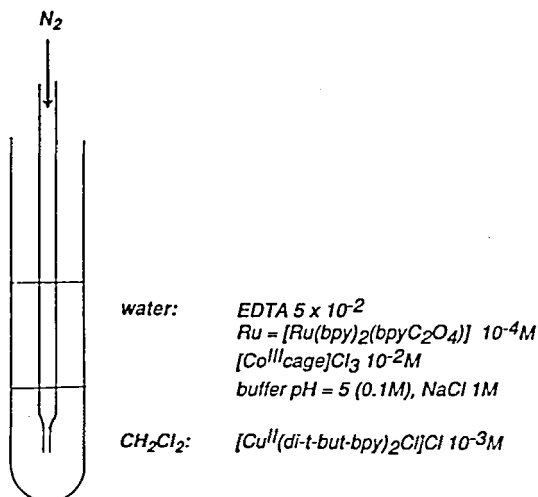


FIGURE 18 Experimental details of the *light driven* two-phase reduction of  $[Cu^{II}(bipyridine)_2Cl]Cl$  in a  $CH_2Cl_2$  layer.

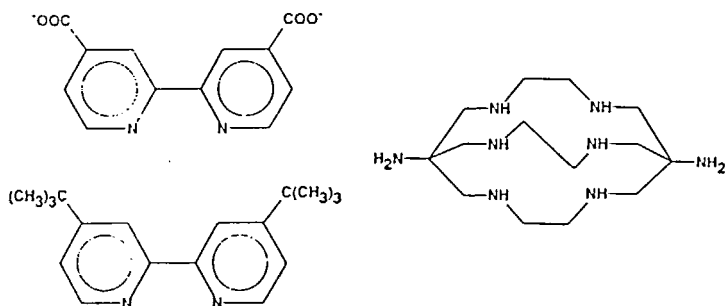
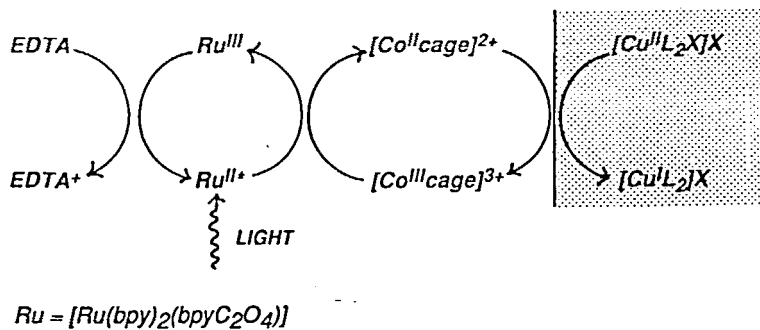


FIGURE 19 Scheme for the *light driven* two-phase reduction of  $[Cu^{II}(bipyridine)_2Cl]Cl$ .

on colloidal platinum from an aqueous solution, under visible light irradiation.<sup>18</sup> In the present case, we use light to generate a quite powerful aqueous reducing agent,  $[\text{Co}^{\text{II}}(\text{diamsar})]^{2+}$ , which is able to transfer electrons, at the water/membrane interface, to the lipophilic oxidizing agent  $[\text{Cu}^{\text{II}}\text{L}_2\text{X}]\text{X}$ . The very true electron source is EDTA;  $[\text{Ru}^{\text{II}}(\text{bipy})_2(\text{bipyC}_2\text{O}_4)]$ ,  $[\text{Co}^{\text{III}}(\text{diamsar})]^{3+}$  and light simply mediate the electron transfer to  $[\text{Cu}^{\text{II}}\text{L}_2\text{X}]\text{X}$ . It should be noted that aqueous EDTA itself, in the same experimental conditions, but in absence of the  $\text{Ru}^{\text{II}}$  complex and/or of the  $\text{Co}^{\text{III}}$  cage complex, does not reduce under two-phase conditions  $[\text{Cu}^{\text{II}}\text{L}_2\text{X}]\text{X}$  (but it reduces, for instance, the more oxidizing lipophilic agent  $[\text{Fe}^{\text{III}}\text{L}_3](\text{ClO}_4)_3$ ). It should be finally mentioned that we used the  $[\text{Ru}^{\text{II}}(\text{bipy})_2(\text{bipyC}_2\text{O}_4)]$  complex, rather than the classical  $[\text{Ru}^{\text{II}}(\text{bipy})_3]^{2+}$  species, for solubility reasons. As a matter of fact,  $[\text{Ru}^{\text{II}}(\text{bipy})_3]^{2+}$  partitions between the aqueous layer and the  $\text{CH}_2\text{Cl}_2$  layer, thus creating a terrible mess. The  $[\text{Ru}^{\text{II}}(\text{bipy})_2(\text{bipyC}_2\text{O}_4)]$  complex, due to the presence of the two negatively charged carboxylate groups, is confined in the aqueous solution. The presence of the  $-\text{COO}^-$  functions does not substantially alter the photophysical properties of the complex.

The above preliminary findings seemed very encouraging and promising for the design of light driven electron transport experiments. However, when performed in the typical conditions we use for transport experiments, the light assisted two-phase reduction of  $[\text{Cu}^{\text{II}}\text{L}_2\text{X}]\text{X}$  appeared extremely slow. In particular, when we filled the 1 cm spectrophotometric cuvette with  $2.0\text{ cm}^3$  of a  $\text{CH}_2\text{Cl}_2$  solution  $5 \times 10^{-4}\text{ M}$  in  $[\text{Cu}^{\text{II}}\text{L}_2\text{X}]\text{X}$  and with  $1.0\text{ cm}^3$  of an aqueous solution containing all the ingredients mentioned before and we illuminated the cuvette from the top, putting the lamp at less than 5 cm from the cuvette, we did not observe any substantial decrease of the absorption band of the  $\text{Cu}^{\text{II}}$  complex, even after one hour. However, slowness of the process does not seem to have any photochemical reason, but it should be simply related to the kinetics of the electron transfer process involving  $[\text{Co}^{\text{II}}(\text{diamsar})]^{2+}$  and  $[\text{Cu}^{\text{II}}\text{L}_2\text{X}]\text{X}$  at the water/dichloromethane interface. As a matter of fact, the same behaviour (no apparent reaction inside the cuvette) was observed using the aqueous  $[\text{Co}^{\text{II}}(\text{diamsar})]^{2+}$  complex generated through cathodic reduction of the  $[\text{Co}^{\text{III}}(\text{diamsar})]^{3+}$  complex. The two-phase process is accelerated, to be complete in a few minutes, if the two immiscible layers are vigorously shaken, manually or by bubbling dinitrogen.

The reason of the sluggishness of the electron transfer process from the  $[\text{Co}^{\text{II}}(\text{diamsar})]^{2+}$  complex, compared to that involving  $\text{Cr}^{\text{II}}$ , can be ascribed to the different stereochemical features of the two reducing agents, which exhibit very close redox potential values.<sup>19</sup> In 1M HCl  $\text{Cr}^{\text{II}}$  should exist as a chloro- or aquo-chlorocomplex: this species is well inclined to interact, somewhere, in the mixed-solvent boundary area, at the water/dichloromethane interface, with the  $[\text{Cu}^{\text{II}}\text{L}_2\text{Cl}]^+$  species. A chloride bridge is probably formed between the two metal centres, which makes the electron transfer from  $\text{Cr}^{\text{II}}$  to  $\text{Cu}^{\text{II}}$  easy and fast, according to a classical inner sphere mechanism. The same mechanism cannot be operative with the substitutionally inert  $[\text{Co}^{\text{II}}(\text{diamsar})]^{2+}$  complex, in which the aliphatic shell of the cage ligand prevents from the formation of any anion bridge.

Thus, failure of the light driven electron transport process across the liquid membrane should not be ascribed to the erroneous design of the experiment, but simply to the bad choice of the electron relay system (and perhaps to the rather poor efficiency of the devices we are currently using in our study). In any case, hydrophilic  $\text{Ru}^{\text{II}}$  polypyridine complexes seem promising sensitizers to be used for the light driven

generation of a reducing agent in ESP. It should be noted that light driven transport of electrons and anions across a supported liquid membrane, using proflavine as a sensitizer in the aqueous reducing phase and Vitamine K as an electron carrier, has been described by Lehn in a classical paper several years ago.<sup>20</sup> More recently, similar light driven transport experiments have been carried out, using methylviologen as a sensitizer in the aqueous reducing phase and again Vitamine K as an electron carrier.<sup>21</sup>

Independently upon the success of the experiments of the type described above, it would seem much more convenient to design transport processes in which the sensitizer is inside the membrane, rather than in one of the two aqueous phases. For instance, a  $[\text{Ru}^{\text{II}}(\text{bipy})_3]\text{X}_2$  complex in the membrane should be excited upon irradiation to the transient form  $^*[\text{Ru}^{\text{II}}(\text{bipy})_3]\text{X}_2$ . The excited state, which displays enhanced reducing and oxidizing properties, should be able to react at the membrane/water interface with aqueous redox agents, thus generating effective charge separation at the two sides of the membrane. In this perspective, we performed some two-phase experiments involving ruthenium(II) 4,4'-di-*tert*-butyl-2,2'-bipyridine ( $\text{L}^1$ ) complexes. However, a  $\text{CH}_2\text{Cl}_2$  solution of  $[\text{Ru}^{\text{II}}\text{L}_3^1](\text{ClO}_4)_2$ , irradiated by a lamp, does not react with an aqueous solution containing  $[\text{Co}^{\text{III}}(\text{NH}_3)_5\text{Br}]^{2+}$ , even under vigorous stirring.  $[\text{Ru}^{\text{II}}(\text{bipy})_3]^{2+}$  assisted photodecomposition of  $[\text{Co}^{\text{III}}(\text{NH}_3)_5\text{Br}]^{2+}$  in aqueous solution represents one of the most classical examples of light promoted electron transfer in homogeneous conditions.<sup>22</sup> Failure of the same process under two-phase conditions is probably to be ascribed to the typical slowness observed for the electron transfer processes taking place at the water/dichloromethane interface compared to the lifetime of the excited state of the ruthenium(II) tris-bipyridine complexes (some hundreds of nanoseconds). More successful experiments could be probably carried out, if a less primitive sensitizer than plain  $[\text{Ru}^{\text{II}}\text{L}_3^1](\text{ClO}_4)_2$  were used.

## 7. GOING UP AND DOWN ALONG THE MEMBRANE ELECTROCHEMICAL SCALE: METAL CYCLAM COMPLEXES

Let an aqueous solution contain two reducing agents of different strength:  $\text{Red}_1$  (less reducing) and  $\text{Red}_2$  (more reducing). If an oxidizing agent  $\text{Ox}$  in excess concentration is added, in absence of any kinetic effect, both  $\text{Red}_1$  and  $\text{Red}_2$  will be indistinctly oxidized. On the contrary, separating the two aqueous solutions by a redox active liquid membrane and choosing an appropriate electron carrier, it can be possible to oxidize selectively  $\text{Red}_2$  in presence of  $\text{Red}_1$ . This possibility is illustrated in Figure 20.

In particular, a carrier  $\text{C}$  should be chosen, whose potential is intermediate between that associated to the aqueous  $\text{Red}_1^+/\text{Red}_1$  couple and that associated to the  $\text{Red}_2^+/\text{Red}_2$  couple. In these conditions,  $\text{Ox}$  will oxidize  $\text{C}$  to  $\text{C}^+$ ;  $\text{C}^+$  can oxidize under two-phase conditions  $\text{Red}_2$ , but not  $\text{Red}_1$ . In this sense the redox active membrane behaves as an electron filter and opens the way to selective oxidation and reduction reactions. In principle, the oxidizing power of any oxidizing agent (or the reducing power of any reducing agent) can be modulated by varying the potential of the electron carrier dissolved in the membrane.

Let us now consider in which way the redox potential of the carrier can be modulated. First, given a metal centred redox couple  $\text{M}^{(n+1)+}/\text{M}^{n+}$ , its potential can be varied by changing the nature of the ligand; the variation of the potential will be more or less pronounced, depending on how drastic will be the modifications carried

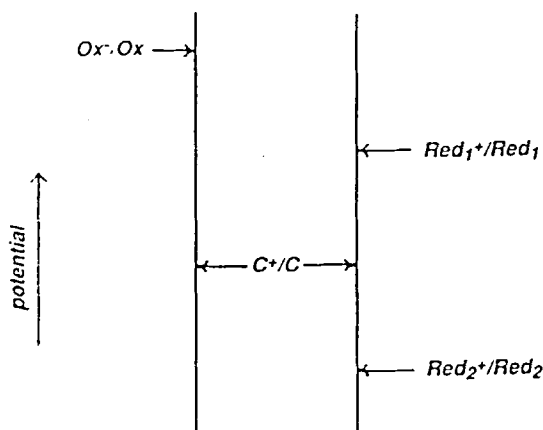
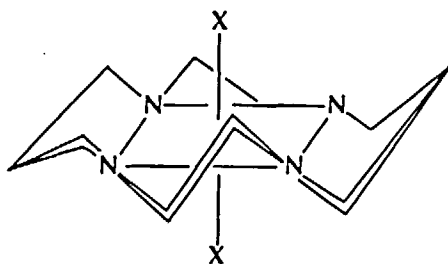


FIGURE 20 The principle of the selective oxidation and reduction reactions using a three-phase device with a redox active liquid membrane.

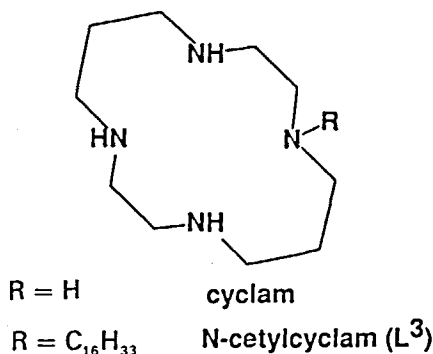
out on the coordinating system. On the other hand, given a chosen ligand, able to promote redox activity of the bound metal centre, serious variations of the electrode potential can be achieved by changing the type of the metal.

We exploited the latter possibility considering 1,4,8,11-tetraza-cyclotetradecane (*cyclam*) as a ligand. *Cyclam* is a very special ligating system for promoting redox activity of the coordinated metal centre and favours the access to oxidation states that are forbidden to the solvated ions or to complexes with less sophisticated ligands.<sup>23</sup> Thus, stable metal complexes in unusually high or low oxidation states have been produced through coordination by *cyclam* or *cyclam*-like molecules:  $\text{Ni}^{\text{III}}$ ,  $\text{Cu}^{\text{III}}$ ,  $\text{Ag}^{\text{II}}$ ,  $\text{Ag}^{\text{III}}$ ,  $\text{Hg}^{\text{III}}$ ,  $\text{Co}^{\text{I}}$ ,  $\text{Ni}^{\text{I}}$ . This property is essentially kinetic in origin: when a metal centre is trapped inside the macrocyclic ring, its reactivity towards exotic redox reagents present in solution, including the solvent, is strongly reduced, so it can persist for a long time. *Cyclam* complexes, typically present a distorted octahedral structure: the macrocycle spans the equatorial plane, whereas two anions  $\text{X}^-$  occupy the axial sites: the axially coordinate anions may act as a bridge for the electron transfer to and from the encircled metal centre.

Thus, *cyclam* complexes represent a class of substitutionally inert metal centred redox systems, prone to an uncomplicated and fast one-electron exchange: they seem ideal candidates to the role of carriers of electrons across liquid membranes.







A lipophilic version of *cyclam* can be easily obtained through reaction of 1-bromo-hexadecane with excess *cyclam*; 1-hexadecyl-1,4,8,11-tetraza-cyclotetradecane (*N*-cetylcyclam,  $L^3$ ) forms complexes with 3d metal ions which are soluble in apolar or poorly polar solvents (benzene, chloroform, dichloromethane, etc.) and completely insoluble in water.<sup>24</sup> In particular, we considered, for transport purposes, two redox couples which situate in opposite parts of the electrochemical scale:  $Ni^{III}/Ni^{II}$ <sup>25</sup> and  $Co^{III}/Co^{II}$ .<sup>26</sup>

In the case of nickel, we prepared the  $Ni^{II}$  complexes and we did, as usual, preliminary investigations of two-phase redox processes. We expected that the  $Ni^{III}/Ni^{II}$  redox couple inside the *N*-cetylcyclam ring should situate in the higher part of the electrochemical scale in  $CH_2Cl_2$ , thus requiring strong aqueous oxidizing agents to carry out the two-phase oxidation to the  $Ni^{III}$  state. In particular, the only efficient aqueous oxidizing agent we found was  $S_2O_8^{2-}$ . Moreover, we observed that the aqueous phase should have a chloride background. The two-phase process is outlined in Figure 21.

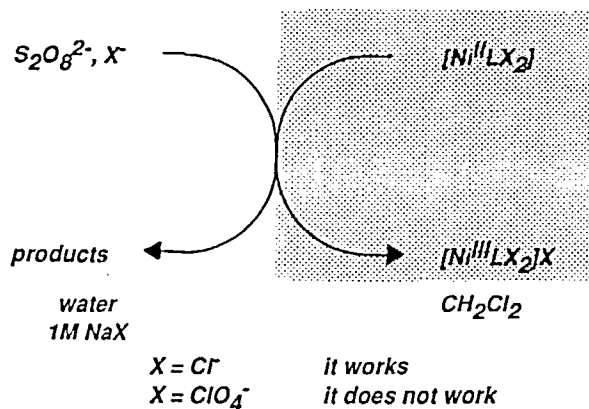


FIGURE 21 Scheme of the two-phase oxidation of  $[Ni^{II}(N\text{-cetylcyclam})X_2]$  by aqueous  $S_2O_8^{2-}$  in presence of a 1 M NaX background. The oxidation is controlled by the nature of the  $X^-$  anion.

The high-spin  $[\text{Ni}^{\text{II}}\text{L}^3\text{Cl}_2]$  complex, pale violet in colour, is oxidized, under two-phase conditions, to the yellow-green  $[\text{Ni}^{\text{III}}\text{L}^3\text{Cl}_2]\text{Cl}$  species. However, if the  $\text{CH}_2\text{Cl}_2$  layer contains the low-spin perchlorate complex,  $[\text{Ni}^{\text{II}}\text{L}^3(\text{ClO}_4)_2]$ , and the aqueous background is  $\text{NaClO}_4$ , no two-phase oxidation takes place, even after prolonged and vigorous shaking. An explanation for this behaviour comes from the voltammetric investigation: the oxidation of  $[\text{Ni}^{\text{II}}\text{L}^3\text{Cl}_2]$  to  $[\text{Ni}^{\text{III}}\text{L}^3\text{Cl}_2]\text{Cl}$  at the platinum electrode in a  $\text{CH}_2\text{Cl}_2$  solution, made 0.1 M in  $\text{Bu}_4\text{NCl}$ , at  $25^\circ\text{C}$ , takes place at a potential of 0.18 V vs  $\text{Fc}^+/\text{Fc}$ . On the other hand, the oxidation of  $[\text{Ni}^{\text{II}}\text{L}^3(\text{ClO}_4)_2]$  to  $[\text{Ni}^{\text{III}}\text{L}^3(\text{ClO}_4)_2]\text{ClO}_4$  at the platinum electrode in a  $\text{CH}_2\text{Cl}_2$  solution, made 0.1 M in  $\text{Bu}_4\text{NClO}_4$ , at  $25^\circ\text{C}$ , takes place at a much more positive potential: 0.92 V vs  $\text{Fc}^+/\text{Fc}$ . In other words, the  $\text{Cl}^-$  anion has a very large stabilizing effect on  $\text{Ni}^{\text{III}}$ , compared to  $\text{ClO}_4^-$ . This behaviour is expected, considering that  $\text{Cl}^-$  is a stronger donor than  $\text{ClO}_4^-$  and that a higher charged cation (*e.g.*  $\text{Ni}^{\text{III}}$ ) profits from the Ligand Field Energy contribution to a larger extent than the less charged cation ( $\text{Ni}^{\text{II}}$ ). However, the difference between the electrode potentials is spectacularly large: more than 700 mV. This probably depends upon the fact that the species are dissolved in a poorly polar, non-coordinating solvent, something similar to the gaseous phase, where interactions between the ions of opposite charge (the metal centre and the anion) are especially strong.

In any case, the two electrochemical scales, in water and in  $\text{CH}_2\text{Cl}_2$ , should be juxtaposed in such a way that the potential associated to the  $\text{S}_2\text{O}_8^{2-}/\text{SO}_4^{2-}$  couple should be higher than the potential of the  $[\text{Ni}^{\text{III}}\text{L}^3\text{Cl}_2]\text{Cl}/[\text{Ni}^{\text{II}}\text{L}^3\text{Cl}_2]$  couple, but lower than that for the  $[\text{Ni}^{\text{III}}\text{L}^3(\text{ClO}_4)_2]\text{ClO}_4/[\text{Ni}^{\text{II}}\text{L}^3(\text{ClO}_4)_2]$  couple (see Figure 22).  $\text{Fe}^{\text{II}}$ , in 1 M HCl, is able to reduce, under two-phase conditions,  $[\text{Ni}^{\text{III}}\text{L}^3\text{Cl}_2]\text{Cl}$  to  $[\text{Ni}^{\text{II}}\text{L}^3\text{Cl}_2]$ . The same can be done by a series of reducing agents stronger than  $\text{Fe}^{\text{II}}$ :  $\text{Ti}^{\text{III}}$ ,  $\text{Cr}^{\text{II}}$ ,  $[\text{Co}^{\text{II}}(\text{diamsarH}_2)]^{4+}$ , the aqueous layer being in any case 1 M in HCl. Noticeably, the  $\text{I}^-$  anion, which is a stronger reducing agent than  $\text{Fe}^{\text{II}}$ , does not reduce  $[\text{Ni}^{\text{III}}\text{L}^3\text{Cl}_2]\text{Cl}$ , under two-phase conditions. Kinetic investigation on the

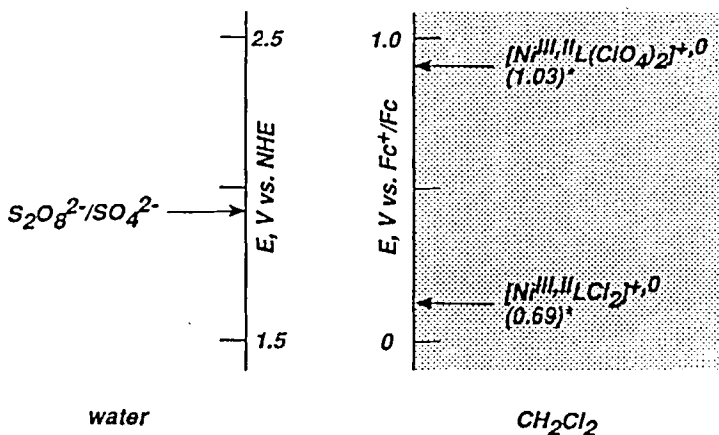


FIGURE 22 Juxtaposition of the electrochemical scale in water (V vs SHE) and of the electrochemical scale in  $\text{CH}_2\text{Cl}_2$  (V vs  $\text{Fc}^+/\text{Fc}$ ), as derived from two-phase redox experiments on the  $[\text{Ni}^{\text{II}}(\text{N-cetyl}(\text{cyclyam})\text{Cl}_2)]/[\text{Ni}^{\text{III}}(\text{N-cetyl}(\text{cyclyam})\text{Cl}_2)\text{Cl}]$  couple.

two-phase redox processes indicated the following rate sequence:



One should consider that in the employed medium (aqueous 1 M HCl) the first three metal ions of the above sequence should exist as chloro- or aquo-chlorocomplexes. It is probable that, in analogy with that mentioned for the two-phase reduction of the  $\text{Cu}^{\text{II}}$  bis-bipyridine complex (*vide infra*), the electron is transferred from the reducing ion to  $\text{Ni}^{\text{III}}$  through a  $\text{Cl}^-$  bridge linking the two metal centres, according to an easy and fast inner-sphere mechanism. This cannot fully explain the sequence of the rates for metal chlorocomplexes, but could at least account for the slowness of the process involving the cobalt(II) cage complex, which, as outlined before, cannot transfer electrons according to this type of mechanism. Moreover, this explains also the failure to react of non metal-centred reducing agents, *e.g.*  $\text{I}^-$ .

Three-phase experiments carried out in the V-shaped glass cell confirmed above findings. Transport experiments were designed in which the excess reagent was  $\text{S}_2\text{O}_8^{2-}$ , 0.1 M in 1 M NaCl. The membrane was  $10^{-3}$  M in  $[\text{Ni}^{\text{II}}\text{L}^3\text{Cl}_2]$ . ESP contained one of the metal-centred reducing agent mentioned before, as limiting reagent ( $10^{-2}$  M) and was 1 M in HCl. When using  $\text{Fe}^{\text{II}}$  as a reducing agent, the progress of the experiment was followed by measuring the concentration of the  $\text{Fe}^{\text{III}}$  chlorocomplex which gradually formed: portions of the ESP solutions were syringed out at regular time intervals; their spectra were measured in a 1 mm quartz cuvette. Plotting absorbance *vs* time data produced the S-shaped profile displayed in Figure 23. Figure 23 shows that after a sort of induction period of about one hour, the concentration of the oxidized form of the aqueous reducing agent increases rather

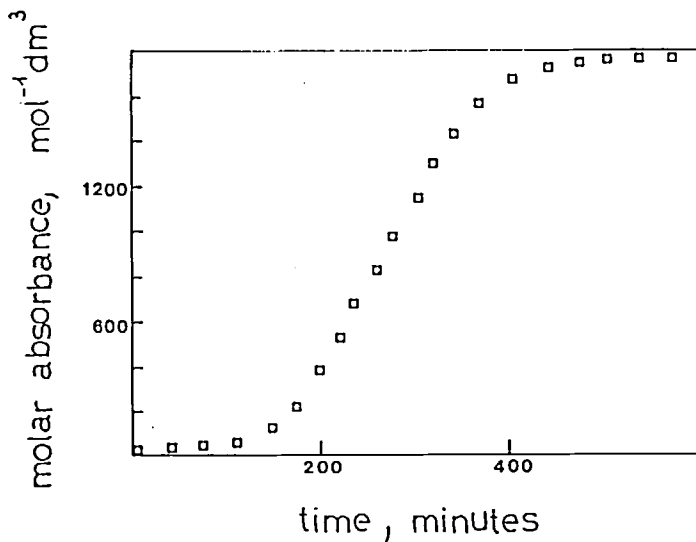


FIGURE 23 Transport profile for a  $\text{S}_2\text{O}_8^{2-}$ ,  $\text{Cl}^-/[\text{Ni}^{\text{II}}(\text{N-cetylcyclam})\text{Cl}_2]/[\text{Ni}^{\text{III}}(\text{N-cetylcyclam})\text{Cl}_2]\text{Cl}/\text{Fe}^{\text{II}}$  experiment. The limiting reagent is  $\text{Fe}^{\text{II}}$  and the progress of the electron transport is monitored through the concentration of its oxidation product,  $\text{Fe}^{\text{III}}$  (as  $\text{FeCl}_4^-$ ).

steeply, to reach a *plateau* after about six hours: at this time all  $\text{Fe}^{\text{II}}$  in ESP has been oxidized and the three-phase redox process is complete. The duration of the experiment is comparable to that observed with electron transport processes mediated by iron(II,III) tris-bipyridine complexes, as described in Paragraph 3. What is unusual is the presence of the induction period. It is probable that this behaviour is related to the special features of  $\text{S}_2\text{O}_8^{2-}$  as an oxidizing agent. We measured the spectra of the membrane during the course of the experiment and we observed that the induction time corresponds exactly to the time necessary for the oxidized form of the carrier,  $[\text{Ni}^{\text{III}}\text{L}^3\text{Cl}_2]\text{Cl}$ , to reach a 50% concentration. It should be recalled that the situation in which both the oxidized and reduced forms of the carrier are at 50% guarantees the higher transport rate. Thus, it is possible that the induction period reflects a sort of autocatalytic pattern necessary to the aqueous  $\text{S}_2\text{O}_8^{2-}$  ion to begin the two-phase oxidation of  $[\text{Ni}^{\text{II}}\text{L}^3\text{Cl}_2]$ . In any case, this slow process takes place at the ERP/membrane interface. When the optimum concentration of the oxidized and reduced forms of the carrier has been reached, the process is controlled by the rate of the two-phase reduction of  $[\text{Ni}^{\text{III}}\text{L}^3\text{Cl}_2]\text{Cl}$  by aqueous  $\text{Fe}^{\text{II}}$ , taking place at the membrane/ESP interface and the typical linear concentration profile is generated. The process outlined is to be classified as of the  $\text{C}/\text{C}^+$  type. The detailed scheme for the electron transport experiments is shown in Figure 24. In the present case, the flow of electrons from ESP to ERP is mediated by a counterflow of chloride ions in the opposite direction.

A similar behaviour was observed for the other metal-centred reducing agents which worked in two-phase experiments. In this case, transferring portions of the ESP solution to the cuvette was not a too safe procedure and we preferred to monitor the concentration of aqueous species in ESP through a potentiometric method. In particular, an indicator electrode (platinum or mercury) and a reference electrode (calomel) were dipped in the ESP compartment (see Figure 25) and potential values were measured at regular time intervals.

Knowing the standard electrode potential associated to the aqueous reducing agent, e.g.  $E^\circ(\text{Cr}^{\text{III,II}}) = -0.65 \text{ V vs SCE}$ , the concentration of the oxidized form (e.g.  $\text{Cr}^{\text{III}}$ ) was calculated through the Nernst equation in its exponential form. Concentration

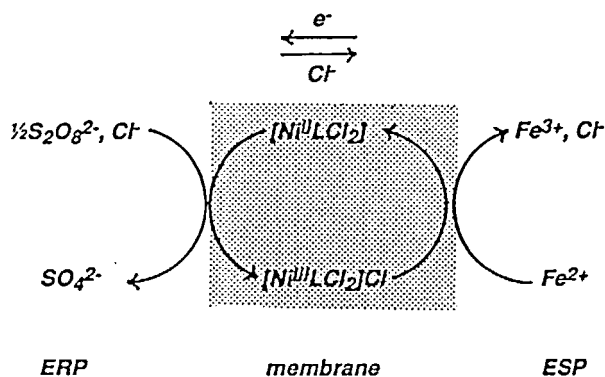


FIGURE 24 Scheme for the transport:  $\text{S}_2\text{O}_8^{2-}$ ,  $\text{Cl}^- / [\text{Ni}^{\text{II}}(\text{N-cetylcyclam})\text{Cl}_2] / [\text{Ni}^{\text{III}}(\text{N-cetylcyclam})\text{Cl}_2]\text{Cl} / \text{Fe}^{\text{II}}$ . The redox system belongs to the  $\text{C}/\text{C}^+$  type and the transport of electrons is coupled to the countertransport of anions  $\text{X}^-$  in the opposite direction ( $\text{X} = \text{Cl}$ ).

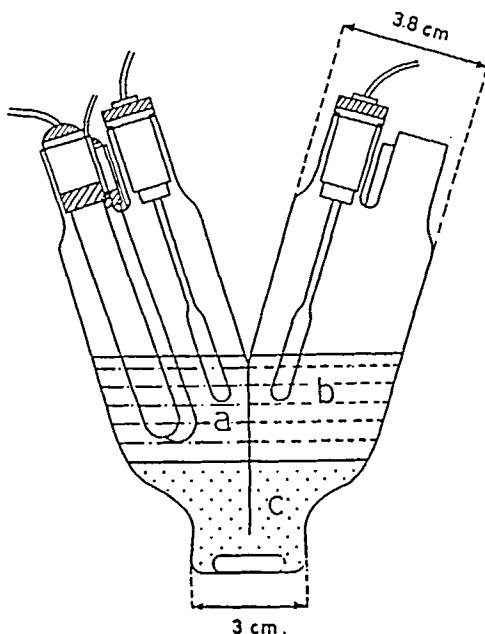


FIGURE 25 V-shaped glass cell used for electron transport experiments involving  $[\text{Ni}^{\text{II}}(\text{N-cetylclam})\text{Cl}_2]$  as an electron carrier. The relative concentration of the aqueous reducing agent and of its oxidized form is monitored through the potential of a platinum or mercury electrode, dipped in the Electron Source Phase. Potential is measured vs a calomel electrode.

vs time plots displayed again a sigmoidal profile. Noticeably, the length of the induction period varied with the different reducing agents: the faster the process (*i.e.* the more positive the slope of the linear portion of the profile), the shorter the length of the induction period. This would indicate that the initial step, probably associated to the activation of peroxydisulfate, should also involve in some way the carrier in its reduced form, at the ERP/membrane interface. Whatever the nature of the mechanism is, results are spectacular: the duration of the electron transport (from the beginning of the experiment to the reaching of the concentration plateau) varies from ten minutes (reducing agent:  $\text{Ti}^{\text{III}}$ ) to twelve hours (reducing agent:  $[\text{Co}^{\text{II}}(\text{diamsarH}_2)]^{4+}$ ), according to the sequence observed in two-phase experiments (see Figure 26).

The  $[\text{Ni}^{\text{III}}\text{L}^3\text{Cl}_2]\text{Cl}/[\text{Ni}^{\text{II}}\text{L}^3\text{Cl}_2]$  redox system is nice and allowed interesting electron transport experiments. As its potential situates in the very anodic part of the  $\text{CH}_2\text{Cl}_2$  electrochemical scale, very strong oxidizing agents are required to generate the  $\text{C}^+$  form. In particular, the only aqueous oxidizing agent we found to work was a very special one: the peroxydisulphate ion, which is known to follow a rather complicated and irreversible reduction pathway. We tried  $\text{Ce}^{\text{IV}}$ , but in  $\text{HClO}_4$  solution it does not oxidize  $[\text{Ni}^{\text{II}}\text{L}_2(\text{ClO}_4)_2]$  under two-phase conditions, probably because its potential situates below that associated to the  $[\text{Ni}^{\text{III}}\text{L}^3(\text{ClO}_4)_2]\text{ClO}_4/[\text{Ni}^{\text{II}}\text{L}^3(\text{ClO}_4)_2]$  couple. On the other hand,  $\text{Ce}^{\text{IV}}$  is not stable in  $\text{HCl}$  solution, being reduced by  $\text{Cl}^-$ , and could not be employed to oxidize  $[\text{Ni}^{\text{II}}\text{L}^3\text{Cl}_2]$ . In any case, keeping  $\text{S}_2\text{O}_8^{2-}$  as an excess reagent, it was possible to explore the behaviour of a wide collection of reducing agents, disclosing some unexpected kinetic effects.

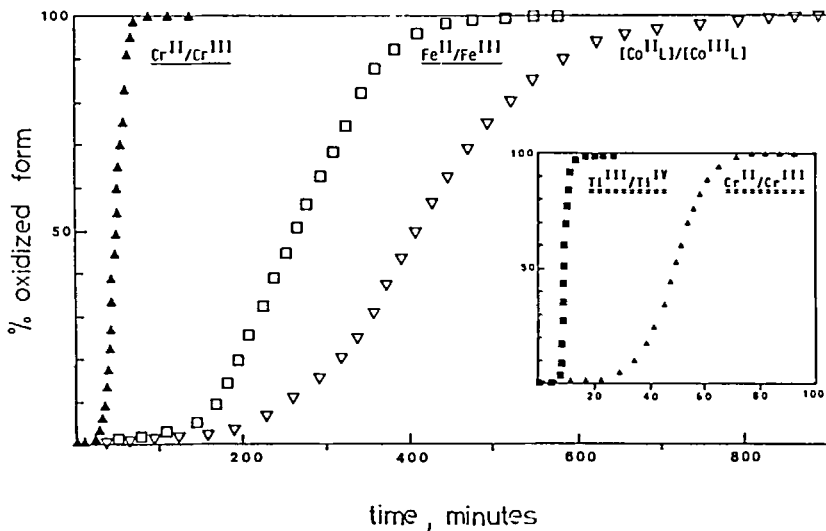


FIGURE 26 Transport profiles for  $S_2O_8^{2-}$ ,  $Cl^-/[Ni^{II}(N\text{-cetyl cyclam})Cl_2]/[Ni^{III}(N\text{-cetyl cyclam})Cl_2]Cl$ /Red experiments (Red =  $Ti^{III}$ ,  $Cr^{II}$ ,  $Fe^{II}$ ,  $[Co^{II}(\text{diansar}H_2)]^{4+}$ ). Each transport has been monitored through the variation of the concentration of the oxidized form of the aqueous reducing agent (limiting reagent).

To look in an analogous way at the behaviour of oxidizing agents, one should move down in the electrochemical scale in  $CH_2Cl_2$ , choosing a redox couple characterized by a rather cathodic electrode potential. In particular, we choose the  $Co^{III}/Co^{II}$  redox change. The green  $[Co^{III}L^3Cl_2]Cl$  complex was prepared through reaction of  $CoCl_2$  with  $L^3$ , in ethanol, in presence of  $O_2$  and  $HCl$ . The potential associated to the  $[Co^{III}L^3Cl_2]Cl/[Co^{II}L^3Cl_2]$  redox change in  $CH_2Cl_2$  solution, 0.1 M in  $Bu_4NCl$ , is  $-0.60\text{ V vs }Fc^+/Fc$ , as measured by the cyclic voltammetry experiment at the platinum microsphere. On the other hand, the  $[Co^{II}L^3Cl_2]Cl$  complex is reduced by aqueous  $Cr^{II}$ , under two-phase conditions, to the divalent species  $[Co^{II}L^3Cl_2]$ , pale pink in colour. The pink  $CH_2Cl_2$  layer, which is extremely air sensitive, can be reoxidized under two-phase conditions, to take again the pristine green colour, through equilibration with a mild oxidizing agent, as  $Fe^{III}$ . Therefore, all the oxidizing agents characterized by a more positive potential than  $0.77\text{ V vs SHE}$  should be able to do the same job. However, the number of such substances is not impressively high, if one looks at one-electron reversible systems.  $Ce^{IV}$ , for instance, cannot be used in presence of  $Cl^-$ , as outlined before. An efficient one-electron oxidizing agent which operates according to an uncomplicated mechanism is  $[Ni^{III}(\text{cyclam})Cl_2]^+$ .<sup>27</sup> This system is completely hydrophilic and, in 1 M  $HCl$ , is a slightly weaker oxidizing agent than  $Fe^{III}$ :  $E(Ni^{III}/Ni^{II}) = 0.73\text{ V vs SHE}$ .

We performed three-phase experiments based on the scheme outlined in Figure 27. The reducing agent,  $Cr^{II}$  0.1 M in 1 M  $HCl$ , was the excess reagent. The membrane was  $5 \times 10^{-4}\text{ M}$  in  $[Co^{III}L^3Cl_2]Cl$ , whereas ESP, 1 M in  $HCl$ , contained  $Fe^{III}$  or  $[Ni^{III}(\text{cyclam})Cl_2]^+$   $5 \times 10^{-3}\text{ M}$ . The decrease of the concentration of the oxidizing agent in ERP was monitored spectrophotometrically. The corresponding profiles are displayed in Figure 28.

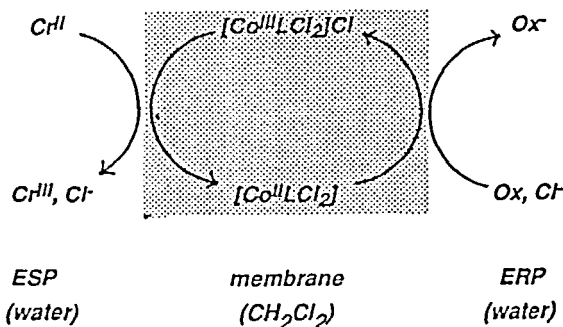


FIGURE 27 Transport scheme for the  $Cr^{II}/[Co^{III}(N\text{-cetylcyclam})Cl_2]Cl/[Co^{II}(N\text{-cetylcyclam})Cl_2]/Ox, Cl^-$  experiment ( $Ox = Fe^{III}, [Ni^{III}(cyclam)Cl_2]^+$ ).

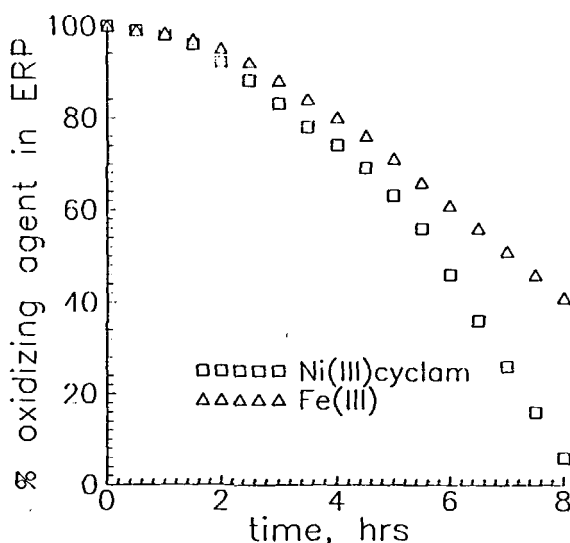
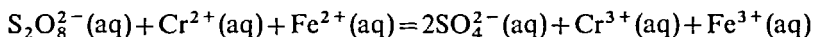


FIGURE 28 Transport profiles for the  $Cr^{II}/[Co^{III}(N\text{-cetylcyclam})Cl_2]Cl/[Co^{II}(N\text{-cetylcyclam})Cl_2]/Ox, Cl^-$  experiment. The transport is monitored through the variation of the concentration of the limiting reagent  $Ox (= Fe^{III}, [Ni^{III}(cyclam)Cl_2]^+)$ .

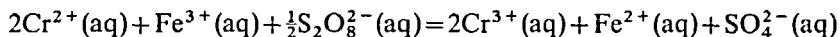
A very short induction period is observed also in the present transport experiments. In this case, however, it should simply reflect the time required for the reduction by  $Cr^{II}$  of the original  $[Co^{III}L^3Cl_2]Cl$  present in the membrane at the beginning of the experiment. After that, a nearly linear decrease is observed for both types of experiments. In this portion, the overall rate is controlled by the process taking place at the membrane/ERP interface. This two-phase process is much faster for  $[Ni^{III}(cyclam)Cl_2]^+$  than for  $Fe^{III}$ . For both aqueous reagents the same type of electron transfer (*i.e.* inner sphere) should operate. There are not elements, at this stage of the investigation, to account for the substantially different rates.

The above data can also be used to illustrate the principle of selective oxidation and reduction reactions using a liquid membrane device, outlined at the beginning of this paragraph. In a first example, let us consider the following redox process in aqueous solution:



The electrochemical scale in water states that peroxydisulphate oxidizes both chromium(II) and iron(II) cations, in homogeneous conditions. However, if the aqueous oxidizing solution and the solution containing the two reducing agents were separated by a  $\text{CH}_2\text{Cl}_2$  layer containing the  $[\text{Co}^{\text{III}}\text{L}^3\text{Cl}_2]\text{Cl}/[\text{Co}^{\text{II}}\text{L}^3\text{Cl}_2]$  system, only chromium(II) ion should be oxidized. As a matter of fact, aqueous  $\text{S}_2\text{O}_8^{2-}$  oxidizes the carrier to its  $\text{C}^+$  form. The oxidized form of the carrier,  $[\text{Co}^{\text{III}}\text{L}^3\text{Cl}_2]\text{Cl}$  oxidizes  $\text{Cr}^{2+}$ , but it has too low a potential to oxidize  $\text{Fe}^{2+}$ , under two-phase conditions (see juxtaposition of the electrochemical scales in Figure 22).

A further example of the use of redox active liquid membranes as an electron filter can be given by the following redox equilibrium:



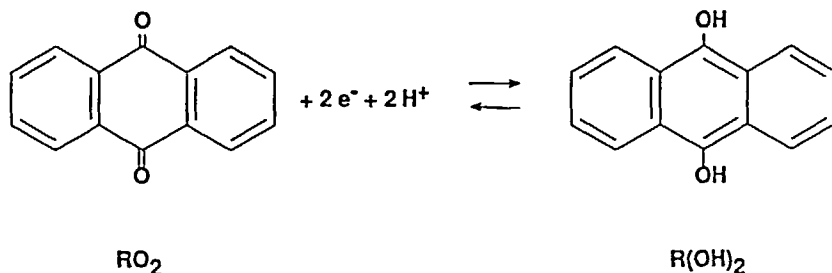
The above homogeneous equilibrium is displaced to the right, as anticipated by the values of the standard potentials in water. However, if a liquid membrane containing the redox system  $[\text{Ni}^{\text{III}}\text{L}^3\text{Cl}_2]\text{Cl}/[\text{Ni}^{\text{II}}\text{L}^3\text{Cl}_2]$  interfaces the solution of the strongly reducing agent  $\text{Cr}^{2+}$  and the solution containing both  $\text{S}_2\text{O}_8^{2-}$  and  $\text{Fe}^{3+}$ , only the strong oxidizing agent  $\text{S}_2\text{O}_8^{2-}$  is reduced, whereas the mild oxidizing agent  $\text{Fe}^{3+}$  persists intact in the solution. Again, the membrane acts as a filter:  $\text{Cr}^{\text{II}}$  transfers electrons to the redox system used as a carrier, stabilizing its reduced form:  $[\text{Ni}^{\text{II}}\text{L}^2\text{Cl}_2]$ . This species is able to transfer electrons to  $\text{S}_2\text{O}_8^{2-}$ , but it has too positive a potential to transfer electrons to  $\text{Fe}^{3+}$ , at the membrane/water interface.

## 8. THE UNSUCCESSFUL DESIGN OF A $\text{C}/\text{C}^-$ REDOX SYSTEM FOR THE CO-TRANSPORT OF ELECTRONS AND PROTONS

Metal complexes with neutral ligands, like *bipy* and *cyclam*, may act as  $\text{C}/\text{C}^+$  carriers and are appropriate for the cross transport of electrons and anions  $\text{X}^-$ , as outlined in the scheme of Figure 7. On the other hand, Figure 6 has shown that, by using a  $\text{C}/\text{C}^-$  redox system, the transport of electrons will be coupled by the co-transport of  $\text{M}^+$  cations. Still using lipophilic metal complexes as carriers, one should consider ligands carrying a negative charge. This route has been chosen by Lehn,<sup>28</sup> who used nickel(II) dithiolene complexes. Dithiolene acts in this case as a bidentate negatively charged ligand:  $\text{D}^-$ . Thus, the half-reaction should be written:  $[\text{NiD}_2] + \text{e}^- = [\text{NiD}_2]^-$ . In that elegant work, the co-transport of cations (i.e.  $\text{K}^+$ ) was controlled by [18]-dibenzo-crown-6, dissolved in the liquid membrane.

A special case arises when the co-transported cation is  $\text{H}^+$ . It should be noted that the transport of hydrogen ions through a membrane driven by a gradient of redox potential is not a scientific curiosity. Nature is playing this game since billions of years. For instance, the transport of protons across the mitochondrial membrane, promoted by *cytochrome c oxidase*, is driven by a gradient of redox potential.<sup>29</sup> The





co-transport of electrons through the metalloprotein takes place *via* a  $\text{Cu}^{\text{II}}/\text{Cu}^{\text{I}}$  redox change. However, the metal centre is coordinated by two cysteinate groups and, looking at the overall electrical change of the active site, the redox change is properly of the  $\text{C}/\text{C}^-$  type.

To realize a co-transport of electrons and protons across a bulk liquid membrane we looked at a much more simple, non metal-centred, redox system: anthraquinone ( $\text{RO}_2$ ). Anthraquinone is able to uptake two electrons and two protons to give the corresponding hydroquinone derivative,  $\text{R(OH)}_2$ . Moreover, both  $\text{RO}_2$  and  $\text{R(OH)}_2$  are soluble in  $\text{CH}_2\text{Cl}_2$  and insoluble in water, fulfilling the first requisite of a redox system for use as an electron carrier. On shaking with an aqueous layer containing  $\text{Cr}^{\text{II}}$  and  $\text{HCl}$ , a  $\text{CH}_2\text{Cl}_2$  colourless layer of  $\text{RO}_2$  takes a bright yellow colour, due to the formation of  $\text{R(OH)}_2$ . This two-phase process was followed inside the spectrophotometric cuvette, in which  $2.0 \text{ cm}^3$  of a  $\text{CH}_2\text{Cl}_2$  solution  $5 \times 10^{-4} \text{ M}$  in  $\text{RO}_2$  and  $1.0 \text{ cm}^3$  of an aqueous solution  $0.1 \text{ M}$  in  $\text{Cr}^{\text{II}}$  and  $1 \text{ M}$  in  $\text{HCl}$  had been stratified. Photons were passed through the magnetically stirred  $\text{CH}_2\text{Cl}_2$  solution. Progress of the two-phase redox process was demonstrated by the decrease of the quinone band centred at  $332 \text{ nm}$  and by the simultaneous increase of the hydroquinone band at  $395 \text{ nm}$ . The decrease of the  $\text{RO}_2$  concentration with the time is illustrated in Figure 29.

The two-phase process appears rather slow, too slow to be "assembled" profitably in a three-phase electron transport experiment carried out in the typical conditions. The slowness of the process seems to be ascribed to the difficulty of the flat and greasy anthraquinone molecule to approach the  $\text{CH}_2\text{Cl}_2/\text{water}$  interface. This consideration prompted us to functionalize the anthraquinone molecule with a subunit which could help the approach to the aqueous medium and to favour the interaction with hydrated species. In this connection, we appended a *cyclam* moiety at one of the lateral rings of anthraquinone.<sup>30</sup> The new conjugate molecule ( $\text{cyRO}_2$ ) binds, through the cyclam ring, 3d metal ions. In particular, we considered the nickel(II) complex:  $[\text{Ni}^{\text{II}}(\text{cyRO}_2)\text{Cl}_2]$ , whose hypothesized stereochemistry is sketched above. This species can be used as a carrier, as it is soluble in  $\text{CH}_2\text{Cl}_2$  and insoluble in water. Moreover it should couple the qualities required by an efficient carrier: (i) capability to uptake electrons and protons of the quinone subunit; (ii) the attitude to interact with polar and hydrated species, through the metallo-cyclam subunit. Preliminary experiments inside the spectrophotometric cuvette were extremely encouraging: the decrease of the quinone band of the  $[\text{Ni}^{\text{II}}(\text{cyRO}_2)\text{Cl}_2]$  complex was extremely fast (see Figure 29) compared to the experiment with plain anthraquinone, performed in the same conditions. This demonstrates the beneficial effect exerted by the  $\text{Ni}^{\text{II}}$ -cyclam subunit in the interaction with hydrated species. However, our

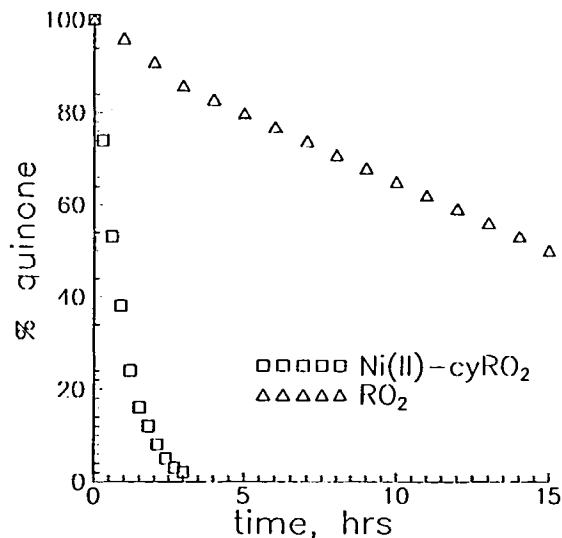
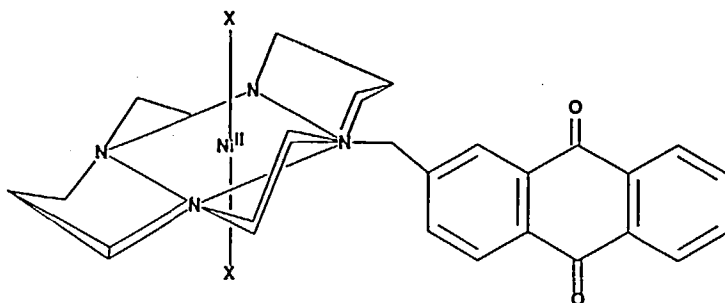


FIGURE 29 Two-phase reduction of the anthraquinone ( $RO_2$ ) fragment by aqueous  $Cr^{II}$ . The progress of the heterogeneous reaction has been monitored through the decrease of the  $RO_2$  concentration. ( $\Delta$ ) anthraquinone; ( $\square$ )  $Ni^{II}$ cyclam-anthraquinone conjugate system.



enthusiasm crashed down when we looked better at the recorded family of spectra in the  $CH_2Cl_2$  layer and we realized that the band relative to the hydroquinone form of the conjugate system,  $[Ni^{II}\{cyR(OH)_2\}Cl_2]$ , was remarkably less intense than expected (about 50%). Thus, we measured the spectrum of the aqueous layer and, from the presence of the hydroquinone absorption bands, we realized that the lost chromophore had left dichloromethane for the aqueous layer. Therefore, the combined effects of the metallo-cyclam subunit and of the two  $-OH$  groups of the hydroquinonic moiety had made the system hydrophilic enough to partition between the two layers. This undesirable property prevents the use of the  $[Ni^{II}(cyRO_2)Cl_2]/[Ni^{II}\{cyR(OH)_2\}Cl_2]$  redox system as a carrier of electrons and protons across a bulk liquid membrane.

A rather obvious and useful synthetic modification of this promising system could be the insertion of a lipophilic group, somewhere in the molecular framework, to

increase hydrophobic properties. We did that, but probably we operated on the wrong portion of the carrier. As a matter of fact, we appended a  $-C_{16}H_{33}$  aliphatic chain on one of the secondary nitrogen atoms of the *cyclam* moiety. However, the two-phase reduction of the quinone fragment of the corresponding  $Ni^{II}$  complex was found even slower than observed with plain anthraquinone, in the same experimental conditions, inside the spectrophotometric cuvette. The reason of this seems rather trivial: by appending the hydrophobic  $C_{16}$  chain on the *cyclam* ring, we nullified the beneficial hydrophilic effects generated by the metal centre and we simply produced a bulkier and greasier carrier than anthraquinone. It is now easy to suggest that the lipophilic functionalization of the conjugate system should be made on the second lateral aromatic ring of anthraquinone. The design of such a molecule is currently pursued in our laboratory.

## 9. CONCLUSIONS AND PERSPECTIVES

The work described before cannot be considered, at this stage, anything more than an amusing scientific game. Its success in the practical applications will depend upon the fortune of liquid membranes as a separation tool. For instance, the two-phase extraction is still a very popular technique for separation or recovery of expensive or precious metals. However, solvent extraction is a bulk and rather primitive technique, which compels to use inexpensive and poorly sophisticated extracting ligands. On the other hand, liquid membrane devices need only a catalytic amount of the extracting ligand, which can be therefore the expensive product of a careful and elaborated synthetic work. As a general rule, the higher the complexity of the ligand, the higher its selectivity in the extraction.

Selective or specific separation of a mixture of metal ions may be made easier by changing in a controlled way the oxidation state and the electrical charge of some desired metal centres. In this sense, the solution of interest, before processing with a conventional metal extracting membrane device, should be pre-treated by an appropriate redox active liquid membrane. Varying the nature of the electron carrier (*i.e.* moving up and down the redox potential of the carrier along the membrane electrochemical scale) may allow to prepare cations in the desired oxidation state for extraction.

The reader needs not to be told that bulk liquid membrane devices of the type described in this review are extremely poor machines and are used only to test, in a relative sense, the chemical efficiency of a designed molecular system. Application should involve much more efficient tools, such as, for instance, supported liquid membranes. In particular, the impregnated hollow fibre technique seems a very promising methodology in the field of separation science and technology.

We mentioned in Paragraph 3 that redox active liquid membranes represent the second multi-phase device to carry out oxidation and reduction reactions keeping the solutions of the reagents separated, the first being the voltaic cell. However, as far as the selective control of redox process is concerned, Volta's device is not so efficient. As a matter of fact, when the half-cell containing one of the redox agents, *e.g.* the reducing agent Red, is opposed to a half-cell containing a mixture of oxidizing agents,  $Ox_1, Ox_2, \dots, Ox_n$ , Red will transfer electrons, through the metal wire, to all the oxidizing agents in the opposed half-cell, in an uncontrolled way, *i.e.* consecutively, according to the sequence of the electrochemical series. In this sense, the three-phase

device based on a redox active liquid membrane is a much more flexible machine: it has been shown in the previous paragraph that in such a device electrons can be filtered at a given potential, putting in the membrane the redox system of the appropriate potential. This allows to stop the redox process after the reduction, or the oxidation, of a wanted species.

Volta's multi-phase machine has had a tremendous impact on science and life, during the last two hundred years. It seems rather hard to forecast a similar success for the three-phase device based on a redox active membrane, discussed in this article. However, before making a final comment, for fairness, one should await, at least, a couple of centuries....

#### ACKNOWLEDGEMENTS

Most of the work described in this review has been supported by the National Council of Research (CNR, Rome: Progetto Finalizzato *Chimica Fine* and *Chimica Fine II*).

#### REFERENCES

1. J.H. Fendler, "Membrane Mimetic Chemistry", Wiley, New York (1982).
2. C.J. Pedersen, *J. Am. Chem. Soc.*, **89**, 7017 (1967).
3. B. Dietrich, J.-M. Lehn and J.-P. Sauvage, *Tetrahedron Letters*, 2889 (1969).
4. J.-M. Lehn, *Angew. Chem. Int. Ed. Engl.*, **27**, 89 (1968).
5. J.-P. Behr, M. Kirch and J.-M. Lehn, *J. Am. Chem. Soc.*, **107**, 241 (1985).
6. M. Di Casa, L. Fabbrizzi, A. Perotti, A. Poggi and R. Riscassi, *Inorg. Chem.*, **25**, 3984 (1986).
7. M. Di Casa, L. Fabbrizzi, A. Perotti, A. Poggi and P. Tundo, *Inorg. Chem.*, **24**, 1610 (1985).
8. L. Fabbrizzi, F. Forlini, A. Perotti and B. Seghi, *Inorg. Chem.*, **23**, 807 (1984).
9. P.R. Danesi, C. Cianetti and E.P. Horwitz, *Solvent Extraction Ion Exch.*, **1**, 289 (1983).
10. A. Volta, *Philos. Trans.*, **2**, 403 (1800).
11. G. De Santis, L. Fabbrizzi, A. Poggi and B. Seghi, *J. Chem. Soc., Dalton Trans.*, **1991**, 1, (1991).
12. J. Mocák and L. Fabbrizzi, unpublished results.
13. E. D. McKenzie, *Coord. Chem. Rev.*, **6**, 186 (1971): [Cu<sup>II</sup>(bipy)<sub>2</sub>X]X.
14. P.J. Burke, K. Henrik, D.R. McMillin, *Inorg. Chem.*, **21**, 1881 (1982): [Cu<sup>II</sup>(bipyridine)<sub>2</sub>X]X and [Cu<sup>I</sup>(bipyridine)<sub>2</sub>]X.
15. *Diamsar*: 1,8-diamino-3,6,10,13,16,19-hexaaza-bicyclo-[6.6.6]eicosane; R.J. Geue, T.W. Hambley, J.M. Harrowfield, A.M. Sargeson and M.R. Snow, *J. Am. Chem. Soc.*, **106**, 5478 (1984); see Figure 19.
16. *bipyC<sub>2</sub>O<sub>4</sub>*: 2,2'-bipyridine-4,4'-dicarboxylate; S. Anderson, E.C. Constable, K.R. Seddon, J.E. Turp, J.E. Baggott and M.J. Pilling, *J. Chem. Soc., Dalton Trans.*, 2247 (1985).
17. A. Juris, V. Balzani, F. Barigelletti, S. Campagna, P. Belser and A. von Zelewsky, *Coord. Chem. Rev.*, **84**, 85 (1988).
18. P.A. Lay, A.W.H. Mau, W.H.F. Saase, I.I. Creaser, L.R. Gahan and A.M. Sargeson, *Inorg. Chem.*, **22**, 2347 (1983).
19. E<sup>o</sup>(Cr<sup>III,II</sup>) = -0.42 V vs SHE; E<sup>o</sup>{[Co<sup>III,II</sup>](diamsar)}<sup>3+,2+</sup> = -0.31 V vs SHE.
20. J.J. Grimaldi, S. Boileau and J.-M. Lehn, *Nature (London)*, **265**, 229 (1977).
21. D.C. Jackman, C.A. Thomas, D.P. Rillema, R.W. Callahan and S.-L. Yan, *J. Membr. Sci.*, **30**, 213 (1987).
22. H.D. Gafney and A.W. Adamson, *J. Am. Chem. Soc.*, **94**, 8238 (1972).
23. L. Fabbrizzi, *Comments Inorg. Chem.*, **4**, 33 (1985).
24. M. Di Casa, L. Fabbrizzi, M. Mariani and B. Seghi, *J. Chem. Soc., Dalton Trans.*, 55 (1990).
25. G. De Santis, M. Di Casa, M. Mariani, B. Seghi and L. Fabbrizzi, *J. Am. Chem. Soc.*, **111**, 2422 (1989).
26. G. De Santis, L. Fabbrizzi, A. Poggi and B. Seghi, *J. Chem. Soc., Dalton Trans.*, 2729 (1990).
27. R.J. Haines and A. McAuley, *Coord. Chem. Rev.*, **39**, 77 (1981).
28. J.J. Grimaldi and J.-M. Lehn, *J. Am. Chem. Soc.*, **101**, 1333 (1979).
29. M. Brunori, G. Antonini, F. Malatesta, P. Sarti and M.T. Wilson, *Eur. J. Biochemistry* **169**, 1 (1988).
30. G. De Santis, L. Fabbrizzi, C. Mangano, A. Poggi and B. Seghi, *Inorg. Chim. Acta* **177**, 47 (1990).